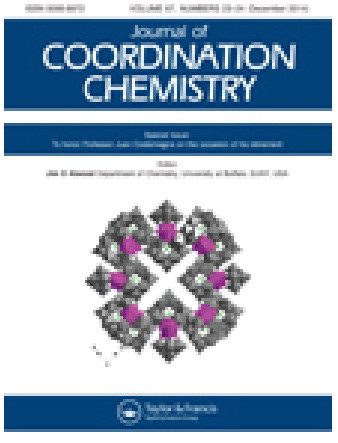

Journal of Coordination Chemistry
Publication details, including instructions for authors and subscription information:
http://www.tandfonline.com/loi/gcoo20

Review: Lanthanide coordination chemistry: from old concepts to coordination polymers

Jean-Claude G. Bünzli[a]
[a] Institut des Sciences et Ingénierie Chimiques, École Polytechnique Fédérale de Lausanne, CH-1015, Lausanne, Switzerland

Accepted author version posted online: 26 Aug 2014.Published online: 25 Sep 2014.

To cite this article: Jean-Claude G. Bünzli (2014) Review: Lanthanide coordination chemistry: from old concepts to coordination polymers, Journal of Coordination Chemistry, 67:23-24, 3706-3733, DOI: 10.1080/00958972.2014.957201

To link to this article: http://dx.doi.org/10.1080/00958972.2014.957201

Journal of Coordination Chemistry, 2014
Vol. 67, Nos. 23–24, 3706–3733, http://dx.doi.org/10.1080/00958972.2014.957201

Review: Lanthanide coordination chemistry: from old concepts to coordination polymers

JEAN-CLAUDE G. BÜNZLI*

Institut des Sciences et Ingénierie Chimiques, École Polytechnique Fédérale de Lausanne, CH-1015, Lausanne, Switzerland

(*Received 3 June 2014; accepted 8 July 2014*)

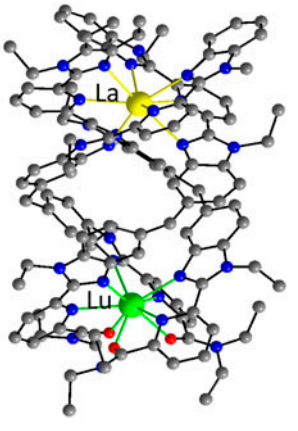

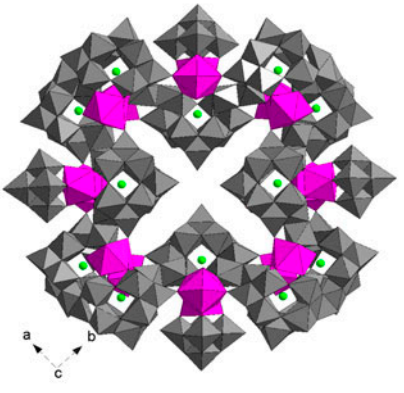

Because of their remarkable and unmatched optical and magnetic properties, the lanthanides are under the limelight when it comes to high technology. These elements are used in strategic applications such as optical glasses and lasers, telecommunications, lighting and displays, magnetic materials, hard-disk drives, security inks and counterfeiting tags, catalysis, biosciences, and medicine, to name but a few. Long considered as minor actors in transition metal chemistry, they have now gained respect from coordination chemists who insert them into sophisticated functional and polyfunctional molecules and materials. This mini review focuses on trivalent lanthanide ions and first summarizes their basic properties. Then some classical aspects of their coordination chemistry are discussed, followed by macrocyclic chemistry, supramolecular chemistry, and self-assembly processes. The last part of this contribution deals with coordination polymers and hybrid materials including potential applications.

Keywords: Lanthanide; Rare earth; Coordination chemistry; Macrocyclic chemistry; Coordination polymer; Self-assembly

*Email: jean-claude.bunzli@epfl.ch

1. Introduction: why bother about lanthanides?

The series of 15 elements from lanthanum (57) to lutetium (71) is commonly referred to as lanthanides or 4f-elements (Ln). According to IUPAC rules though, they should be named "lanthanoids" but this term meets some difficulty in being adopted by scientists. When scandium and yttrium are added, the series takes the name of "rare earths." Group 3 elements (Sc, Y, La, and Ac) are in fact the first elements of their respective d-transition series (3d, 4d, 5d, and 6d). The remaining lanthanides (Ce–Lu) are not seen in the main frame of the periodic table of the elements and they are commonly listed separately at the bottom, essentially for ensuring a more compact layout; this reflects quite well the fact that the name "lanthanide" comes from *lanthanein*, meaning "to escape notice" in Greek. The place of lanthanides in the periodic table of the elements has been and still is the subject of debates and several different periodic classifications have recently been proposed some of them intermingling d- and f-block elements [1].

The first rare earth element or, rather, its sesquioxide yttria, Y_2O_3, was discovered in 1794 and it took a bit more than 100 years to separate and characterize the other non-radioactive rare earths, the last one being lutetium (1907), while radioactive promethium has been synthesized in 1947 [2]. The story is long and full of wrong claims but basically the discoveries benefited from progresses in separation and crystallization techniques on one hand and in atomic spectroscopy on the other hand. Industrial applications had to wait Carl Auer von Welsbach who in addition to separating praseodymium and neodymium from didymium in 1885 invented two products related to lighting: the incandescent mantle for gas lighting in 1891 and the mischmetal in 1903, an essential component of flint stones and used in several metallurgical processes. In 1910, he also introduced lanthanide fluorides into the electrodes of arc lamps for motion-picture studios in order to increase their brilliance. The early industrial period of rare earths ended around 1930 when electricity replaced gas lighting. The second industrial era, between 1930 and 1960, is characterized by new applications, particularly those of cerium oxide as polishing powder and additive in optical glasses – including sunglasses, and in catalysts. In the aftermath of World War II, large quantities of thorium oxide were produced as catalyst in the Fischer–Tropsch process and as feed materials in breeder nuclear reactors; this generated substantial quantities of rare earths which were, however, left over as useless by-products. The situation changed in the early 1960s when atomic programs in the USA and USSR generated abundant rare earths as fission products of nuclear reactors leading scientists to become interested in their properties. Efficient separation processes were developed yielding highly pure rare earth oxides and salts which were then incorporated into more sophisticated applications. One striking example is the red phosphor Y_2O_3 : Eu which was introduced in television screens in 1965. Further optical applications then developed with the advent of lasers in the mid-1960s while catalysts gained momentum too. Diversification of the use of rare earths in high-technology products accelerated in the 1980s with the advent of the erbium-doped amplifier in optical-fiber telecommunications, powerful neodymium–iron–boron magnets, and biomedical applications such as time-resolved immunoassays and contrast agents for magnetic resonance imaging, not to mention security inks and counterfeiting tags. In the twenty-first century, most facets of technology, including defense aspects, depend on rare earths. Yet, apart from magnets and some catalysts or polishing powders, the amount of rare earth(s) in a given product often represents only a small quantity (typically 200 mg in a smart phone) and usually less than a few percent of its price. This feature remained unnoticed until 2010: following geopolitical turmoil between China and Japan, the stunned world realized that

China had a large monopoly on the production (>95% in 2012) and technology of these elements. Military and political staff panicked, prices were multiplied 20–100-fold and mining operations were reopened or newly opened in the western world while dozens of potential mines started to be prospected. At the time of this writing, the crisis is more or less over, but the hefty interest stirred for rare earths remains, several of them being now classified by some governments as strategic elements.

From the scientific point of view, inorganic chemists have long ignored the rare earth elements or, rather, considered them as of minor interest. For instance, in a widely distributed introductory textbook to chemistry published in 1971, it was stated *Lanthanum has only one important oxidation state in aqueous solution, the 3+ state. With few exceptions, this tells the whole boring story about the other 14 lanthanides* [3]. Such an attitude probably stems from the fact that earlier applications were essentially linked to simple inorganic compounds, salts, and oxides, and that solvent extraction methods were based on rather simple organic extractants, such as aminocarboxylic acids (e.g. nta, edta, and dtpa) or alkylphosphoric acids. Two other factors contribute to this poor opinion about lanthanides. Firstly, a modest redox chemistry, restricted to a few elements (Ce^{IV}/Ce^{III}; Ln^{III}/Ln^{II} with Ln = Sm, Eu, Yb), at least until recently since advances in organometallic chemistry have presently extended this redox chemistry to all members of the series [4, 5]. Secondly, owing to the inner nature of the 4f valence orbitals, ligand field effects for the trivalent ions are very small, on the order of 500 cm^{-1} (6 kJ mol^{-1}) while these effects for d-transition metal ions are commonly in the range of 10–30,000 cm^{-1} (120–360 kJ mol^{-1}). Modest interest for the 4f elements is reflected by an 87-page review which appeared in 1979 and which perfectly well covers essential knowledge about coordination and organometallic chemistry of the rare earths [6]. However, in order to keep up with the fast expansion of the field in the 1980s, a wealth of more specialized reviews appeared soon after. The reluctance of chemists to consider rare earth elements as being as interesting as d-transition elements persisted at least until the 1990s when their coordination chemistry was given a lot of renewed attention, fueled by burgeoning applications in catalysis, medicine, and material sciences, thanks to their intriguing spectroscopic and magnetic properties.

The past 25 years have seen the emergence of several exciting areas linked to the coordination chemistry of 4f elements dealing, for instance, with macrocyclic ligands, new extraction processes, self-assembled supramolecular edifices, heterometallic d-f compounds, coordination in ionic liquids, lantanidomesogens, lanthanidofullerenes, nanoparticles, crystal-to-crystal reactions, coordination polymers (CPs), as well as functionalized and host–guest hybrid materials. In parallel, physicochemical studies have shed light on the thermodynamic aspects of the chemical bonding in f-element compounds and theoretical modeling has made substantial advances thanks to the recent availability of relativistic and contracted basis sets for the elements La–Lu optimized for density functional theory applications. These advances make coordination chemistry of the 4f elements a mature and attractive field of research with almost unlimited perspectives. In this contribution, we give a general overview of these developments, specifically excluding organometallic compounds (in the strict sense of the term, i.e. compounds having Ln–carbon bonds) and focusing on the series La–Lu (except Pm) with a bias for luminescent properties. Owing to space restriction we essentially cite review articles.

2. Basic properties of the trivalent ions

Scholarly introductions into the properties of 4f elements and their compounds can be found in Refs. [2, 7, 8]. Abrupt decrease in energy of the 4f orbitals at atomic number 57 results in the progressive filling of these orbitals after La. f orbitals penetrate the xenon core to a substantial degree and are well shielded by the filled 5s, 5p, and 6s (for atoms) sub-shells. As a result, interaction with ligand orbitals is minimum, the bonding in lanthanide complexes is only weakly covalent, the stereochemistry of the complexes is directed by steric properties of the ligands, and ligand-field effects are small; therefore, spectroscopic and magnetic properties are little affected by the environment of the metal ion. Some properties of the lanthanides and their trivalent ions are gathered in table 1. A few important facts in relationship with their coordination chemistry are summarized below. Two introductory books describing fundamental aspects as well as applications of magnetic and luminescent properties of rare earth coordination compounds are useful entries into the field [9, 10].

2.1. *Electronic configurations and ionization energies*

The electronic configuration of the Ln elements is $[Xe]5d^16s^2$ for La; $[Xe]4f^n5d^16s^2$ for Ce ($m = 1$), Gd ($m = 7$), and Lu ($m = 14$); $[Xe]4f^n6s^2$ for Pr–Eu ($n = 3$–7); and Dy–Yb ($n = 9$–14). The most stable, trivalent ions have $[Xe]4f^n$ configuration ($n = 0$–14) and the same is true for divalent and tetravalent lanthanides (with different n of course). The elements are highly electropositive as shown by Pauling's electronegativity data and ionization energies increase along the series with, however, some irregularities. For instance, stabilizing effects of half-filled and filled sub-shells are seen in low I_3 values for Gd and Lu and high I_3 values for Eu and Yb; these trends are also reflected in the cumulative I_{1-3} values, explaining the stabilities of the respective +3 and +2 states of these pairs of elements.

Table 1. Selected properties of lanthanides, yttrium, and their trivalent ions.

Ln	χ_P	I_3	I_{1-3}	$E^0_{r,3-0}$	$E^0_{r,3-2}$	ΔH^0_h	$\log {}^*\beta_{11}$	pH	r_i (6)	r_i (9)	r_i (12)
La	1.10	1850	3455	−2.379	−3.1	−3326	−9.01	7.47	103	122	136
Ce	1.12	1949	3523	−2.336	−2.92(8)	−3380	−10.6	7.10	101	120	134
Pr	1.13	2086	3627	−2.353	−2.84(6)	−3421	−8.55	6.96	99	118	132
Nd	1.14	2130	3694	−2.323	−2.62(5)	−3454	−8.43	6.78	98	116	130
Pm	1.13	2150	3738	−2.30	−2.44(5)	−3482	n.a.	n.a.	97	114	128
Sm	1.17	2260	3871	−2.304	−1.50(1)	−3512	−8.34	6.65	96	113	127
Eu	1.2	2404	4035	−1.991	−0.34(1)	−3538	−8.31	6.61	95	112	125
Gd	1.20	1990	3750	−2.279	−2.85(7)	−3567	−8.35	6.58	94	111	124
Tb	1.1	2114	3790	−2.28	−2.83(7)	−3600	−8.16	6.47	92	110	123
Dy	1.22	2200	3898	−2.295	−2.56(5)	−3634	−8.10	6.24	91	108	122
Ho	1.23	2204	3924	−2.33	−2.79(6)	−3663	−8.04	6.20	90	107	121
Er	1.24	2194	3934	−2.331	−2.87(8)	−3692	−7.99	6.14	89	106	119
Tm	1.25	2285	4045	−2.319	−2.22(5)	−3717	−7.95	5.98	88	105	118
Yb	1.1	2415	4194	−2.19	−1.18(1)	−3740	−7.92	5.87	87	104	117
Lu	1.27	2033	3896	−2.28	n.a.	−3759	−7.90	5.74	86	103	116
Y	1.22	1980	3777	−2.372	n.a.	−3640	−8.36	n.a.	90	108	n.a.

Notes: Key: χ_P = Pauling's electronegativity; I_3 = third ionization energy (rounded to 1 kJ mol^{-1}) [8]; I_{1-3} = sum of the first three ionization energies (rounded to 1 kJ mol^{-1}) [8]; $E^0_{r,3-0}$ = standard redox potential Ln^{+3}/Ln^0 in V at pH 0 [12]; $E^0_{r,3-2}$= redox potential Ln^{+3}/Ln^{+2} in V [13], value for La is calculated; ΔH^0_h = standard hydration enthalpies in kJ mol^{-1} calculated by semi-empirical methods (Born–Haber cycles) [14]; $*\beta_{11} = [(LnOH)^{2+}][H^+]/[Ln^{3+}]$, ionic strength = 0.3 M [15]; pH = pH at which hydroxide precipitation starts in $Ln(NO_3)_3$ solutions 0.1 M in water [16]; $r_i(n)$ = ionic radii for coordination numbers $n = 6$, 9, and 12 in pm [17].

2.2. *Hydration enthalpies, hydrolysis constants, and anion complexation*

Hydration enthalpies are large and increase with increasing atomic number. This means that complexation in water must overcome the desolvation energy and therefore strongly coordinating ligands are required for tailoring highly stable complexes. Since Ln^{III} ions have hard Lewis acid character, hard bases are usually preferred, such as carboxylates, generating strong ionic bonds. In addition, stabilization of the complexes is commonly achieved with large favorable entropic effects generated by multidentate ligands. Another delicate point is the high stability of hydroxy species, compared to $\log {}^{*}\beta_{11}$ values and pH values at which precipitation starts to occur in water. This limits somewhat the pH range in which one may operate during complexation. In non-aqueous media, solvation remains a prevalent phenomenon, especially in solvents with large donor numbers like DMSO and DMF. Therefore, extreme care has to be exercised when dissolving a lanthanide complex in these solvents which easily dissociate ligands. In water, simple anion complexation does not really compete with ligand binding. On the other hand, this is no more the case in non-protic solvents, even for "non-coordinating" anions such as perchlorate and triflate: in 0.05 M solutions in acetonitrile, for instance, the main solvated species are $[Ln(NO_3)_3(MeCN)_x]$, $[Ln(SO_3CF_3)_2(MeCN)_x]^+$, and $[Ln(ClO_4)(MeCN)_x]^{2+}$ [11].

2.3. *Ionic radii and coordination numbers*

Lanthanides ions have large ionic radii and can therefore accommodate large coordination numbers. The ionic radii sustain a progressive and rather smooth decrease (disregarding second-order effects) with increasing atomic number, that is with increasing charge density, resulting in the so-called "lanthanide contraction". The ionic radii in the middle of the Ln series are similar to those of Ca^{II}. Ionic radii strongly depend upon coordination numbers: differences between coordination numbers 6 and 12 amount to about 30 pm, which makes Ln^{III} ions highly adaptable to many coordination environments.

The geometrical arrangement around the lanthanide ions basically depends upon the steric properties of the ligands, so that suitable design of the ligating molecules leads to easy tuning of their coordination numbers. As a matter of fact, in crystals, coordination numbers between 3 and 12 are documented, the former with bulky ligands such as bis(trimethylsilyl) amine, the latter with small bidentate ligands such as nitrate and/or macrocyclic ligands. A study conducted on 1389 structurally characterized Ln^{III} and Y^{III} coordination compounds reported between 1935 and 1995 reveals that coordination numbers 8 and 9 are by far the most frequent (figure 1). Coordination number 6 represents a special historical case. Despite the crystal structure of $[Nd(H_2O)_9](BrO_3)_3$ had been determined in 1939 already and clearly pointed to nine coordination, a commonly expressed opinion was that the rare earth ions formed six-coordinate, octahedral complexes similarly to 3d-transition metals. Work on polyaminocarboxylate complexes of yttrium and cerium by the group of G. Schwarzenbach in the early 1960s started casting doubt on this thinking. The six-coordinate theory finally faded out in 1965 when the structures of complexes with ethylenediaminetetraacetic acid, $NH_4[La(edta)(H_2O)_3]\cdot 5H_2O$ and $[La(Hedta)(H_2O)_4]\cdot 3H_2O$, pointed to La^{III} being 9- and 10-coordinate, respectively [6]. The most representative examples of six-coordination are elpasolites containing $[LnX_6]^{3-}$ hexahalide anions.

The coordination polyhedra commonly deviate from the idealized symmetrical structures of lowest energy calculated on the basis of n identical Ln–ligand bonds and deviation usually increases with ligand complexity. Complexes with small monodentate ligands tend to

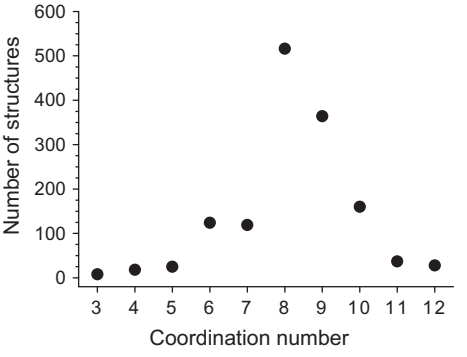

Figure 1. Distribution of coordination numbers among rare earth complexes (La–Nd, Sm–Lu, Y) as evidenced from 1389 crystal structures published between 1935 and 1995 [9].

have similar solid-state structure along the Ln series as exemplified by nine-coordinate hydrates $[Ln(H_2O)_9]^{3+}$, which all display face-centered (tricapped) trigonal prismatic (TTP) geometry with idealized D_{3h} symmetry. It is important to realize that for large coordination numbers the energy of reorganization in going from one polyhedron to another, or even, in solution, in going from one coordination number to the next one by addition of a solvent molecule, is fairly small. Coordination environments are usually assigned to an ideal polyhedron using the shape measure metric *S(δ,θ)* which compares dihedral angles between the normals to adjacent binding faces of the polyhedron in the crystal structure (δ_i) with those of the ideal polyhedron θ_i for the m edges of the polyhedron [18]:

$$S(\delta,\theta) = \min\sqrt{\frac{1}{m}\sum_{i=1}^{m}(\delta_i - \theta_i)^2} \tag{1}$$

Alternatively, the continuous symmetry method (CSM) compares distances between vertices of the experimental and idealized polyhedra. Similarly to the previous method, the polyhedron closest to the experimental one can be determined but, in addition, the CSM concept allows one to define the symmetry content in a given structure. This can be quite useful in interpreting spectroscopic data for species with pseudo-symmetry [19, 20]:

$$S(P,Q) = \min\frac{\sum_{i=1}^{N}(Q_i - P_i)^2}{\sum_{i=1}^{N}(Q_i - Q_0)^2} \tag{2}$$

where Q_i and P_i are the coordinates of the vectors defining the N vertices of the experimental and idealized polyhedra, respectively, while Q_0 is the coordinate vector of the center of mass of the investigated structure; therefore, *S(P,Q)* lies between 0 and 1.

Owing to the high lability of the Ln^{III} ions, solutions frequently contain a mixture of species. A scholarly example is the aqua ions $[Ln(H_2O)_n]^{3+}$: in the solid state, all bromates and ethylsulfates are nine coordinate [14] with a fairly regular TTP coordination geometry; in solution, however, the coordination number decreases gradually from nine at the beginning of the series to eight at the end, with fractional numbers indicating equilibria between eight- and nine-coordinate species [21].

2.4. *Kinetics aspects*

Ln^{III} ions are highly labile as shown by water dissociation rates depicted in figure 2 for the following reaction [22]:

$$[LnSO_4(H_2O)_n]^{2+} \overset{k_d}{\rightleftarrows} [LnSO_4(H_2O)_{n-1}]^{2+} + H_2O \quad (3)$$

This is also true for non-aqueous solutions; for instance, the rates for DMF exchange are in the range $0.4–9.9 \times 10^7\ s^{-1}$ at 298 K [23] for the heavier lanthanides (Tb–Yb). Lability of complexes spans a large range, ligand exchange being fast for monodentate ligands but increasingly slow for polydentate ones, e.g. $k_f = 7.7 \times 10^{-2}\ s^{-1}$ for $[Lu(dtpa)]^{2-}$ [24]. In some specific cases, complexes may become even more inert, for instance, complexes with macrocyclic ligands, particularly dota ($k_f \sim 10^{-4}\ s^{-1}$ for $[Lu(dota)]^-$ [24]). It is to be stressed here that kinetic inertness and thermodynamic stability are equally important when it comes to the applications of lanthanide complexes to *in vivo* bioimaging [25].

3. Classical aspects of lanthanide coordination chemistry

The coordination chemistry of lanthanide inorganic compounds is well understood and is summarized in several books and review articles [9, 10, 26–28]. This category of compounds also includes polyoxometalates [29, 30] and cluster compounds [31]. As outlined above, most organic molecules used to tailor Ln^{III} complexes are polydentate ligands and historically speaking, carboxylates and polyaminocarboxylates have played an important role, particularly with respect to extraction and separation of lanthanides [32]. The superiority of polydentate ligands over mono or bidentate ones is exemplified in figure 3: dtpa complexes are about 20 orders of magnitude more stable than acetates. It is noteworthy that a linear correlation is obtained when $\log K_1$ values are plotted *versus* the sum of the pK_a of

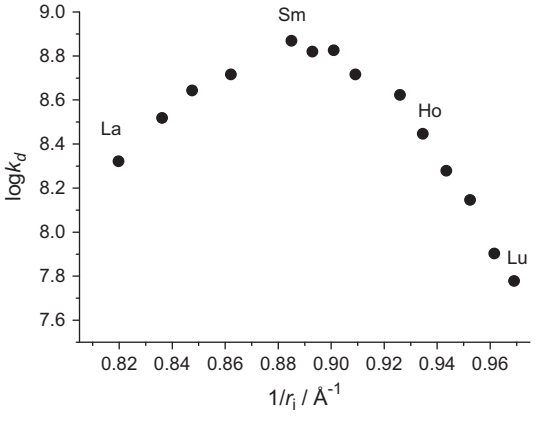

Figure 2. Water dissociation rates (298 K) *vs.* inverse ionic radii for coordination number 9. Drawn from data in [22].

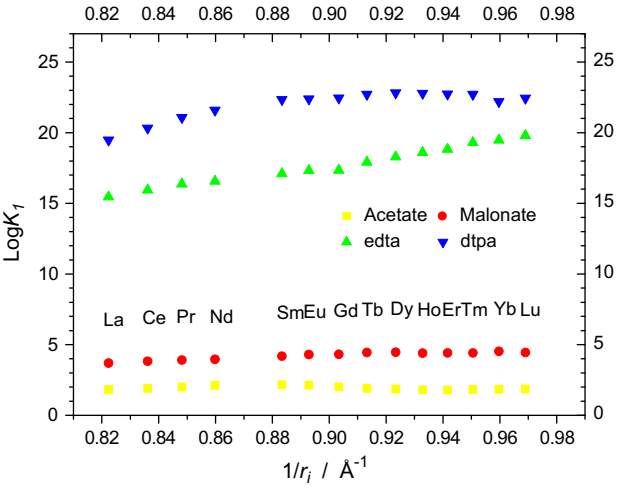

Figure 3. Stability constants for the formation of 1:1 complexes in water at 298 K *vs.* reciprocal ionic radii for coordination number 9. Drawn from data in [33].

the ligands and that ligands inducing the formation of five-membered chelate rings lead to more stable complexes.

Another large class of lanthanide complexes features β-diketonates. Although not particularly stable in water, they are ubiquitous in luminescence applications such as sensitive elemental analyses and bioanalyses, electroluminescent layers for organic light-emitting diodes, visualization of fingerprints, security inks, mechanoluminescent coatings, or polymeric waveguide amplifiers. They have also been used as shift reagents in NMR spectroscopy, in rare earth separation by gas chromatography, and as catalysts in Diels–Alder reactions [34]. Several types of complexes are available: (i) anhydrous tris complexes, (ii) hydrated or ternary tris complexes in which the coordination sphere is saturated by an ancillary ligand, which allows one to finely tune luminescence properties, (iii) anionic tetrakis complexes [34], (iv) bis(diketonates) that have been used in bioanalyses [35] and, more recently, (v) tetrakis(β-diketone) podates which have the advantage of generating a large chelate effect [36].

Although approximately 40% of the complexes for which structural data are available contain Ln–O bonds only and altogether 75% contain at least one Ln–O bond, bonding to nitrogen donors is also important since 25% of lanthanide complexes contain at least one Ln–N bond [9]. This shows that preference for oxygen donors is only one factor among others influencing the stability of rare earth complexes. As a matter of fact, aliphatic amides, silylamides, pyridine- or benzimidazole-based ligands, porphyrins, phthalocyanines, and Schiff base ligands are interesting building blocks for the design of complexes and associated materials with specific magnetic and/or optical properties [37]. Compartmental Schiff bases, both acyclic and, more important, macrocyclic, have played and are still playing a decisive role in lanthanide coordination chemistry because they open the way for polynuclear edifices encompassing both f- and d-transition ions [38].

Compounds with S, Se, or Te donor atoms are rarer, although complexes with polythiophenes and tetrathiafulvalene derivatives [39] as well as chalcogenide clusters [40] generate interesting optical and/or single-molecule magnet properties.

4. Macrocyclic chemistry

4.1. *Initial studies*

In classical coordination chemistry of rare earths, selectivity between two members of the series essentially depends on differences in charge density of the cations, which leads to small changes only in the associated stability constants (see figure 3). When macrocyclic chemistry based on host–guest (supramolecular) interactions developed in the 1980s, there has been hope that more selectivity could be induced within the lanthanide series. Several classes of ligands, crown ethers, aza-crown ethers, cryptands (chart 1), calixarenes, cyclic Schiff bases, porphyrins, phthalocyanines, and metallacrowns were investigated [10, 41]. Two types of philosophy underline these studies.

The first one is the lock-and-key concept in which the ligand cavity is adjusted to the ionic diameter of the metal ion. The principle works well when it comes to differentiate say sodium from potassium or calcium, but not when two different Ln ions are implied. Indeed, tuning of the preorganized ligand cavity is too coarse with respect to the minute differences in ionic radii. In fact, comparison of stability constants with cryptands (2.1.1), (2.2.1), and (2.2.2) in various solvents shows that if indeed the cavity size matters, (2.2.1) being best adapted to Ln^{III} ions, stability is essentially governed by solvent effects. This statement is also valid for coronates [42].

The second, induced-fit principle uses flexible ligands, e.g. small macrocycles fitted with pendant coordinating arms, or podands, which are able to adjust their coordinating cavity to the guest ion. Undoubtedly, this works better for lanthanides, leading to more stable complexes but since the ligand can finely adjust to the size of the metal ion, even less discrimination between consecutive lanthanides is obtained compared to the "lock-and-key" ligands. Figure 4 illustrates these points: (i) while stability constants of 1 : 1 complexes with 15-crown-5 and 18-crown-6 ethers indeed display some size discrimination, they remain small; (ii) replacing two ether functions with amine groups to yield the more flexible (2.1) and (2.2) coronands increases the stability by 7–8 orders of magnitude, but selectivity is reduced.

That (2.2) is a more flexible ligand compared to 18C6 is seen in the top panel of figure 5 which, in addition, exemplifies the similarity of the ligand wrapping around the metal ion between a coronand and a podand with the same type and number of donor atoms. When cyclen is grafted with acetic acid groups in H_4dota, the induced-fit principle deploys all its efficiency and the resulting complexes are the most stable known for Ln^{III} ions (bottom panel, figure 5). Therefore, except in rare cases, macrocyclic ligands have not provided a general solution to a better separation of lanthanides; counter examples are a lariat ether in which the amine function of aza-15C5 is grafted with a $MeO(CH_2)_2$-group, leading to selective complexation of Nd^{III} [42] or (2.1)DA resulting from the attachment of two acetic acid functions onto the amine groups of (2.1) and displaying a peak of selectivity for the middle Ln^{III} ions (Ln = Nd–Tb) [10].

4.2. *Main classes of macrocyclic complexes*

Because they provide a protective multidentate environment for the lanthanide ions, and, more importantly, because their framework can be derivatized at will to generate multifunctional entities, a wealth of macrocyclic complexes has been designed and studied. The most prolific class of such compounds is made of the coronates based on cyclen derivatives

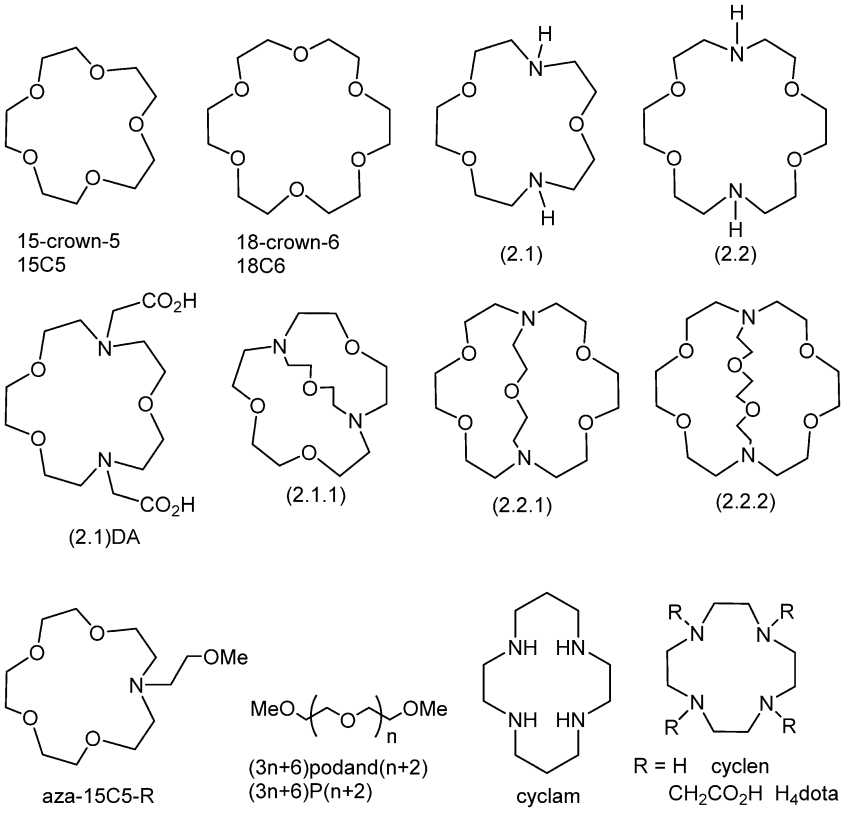

Chart 1. Simple coronands, cryptands, and podands.

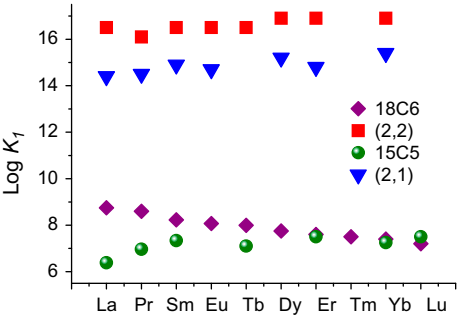

Figure 4. Stability constants of 1:1 coronates in propylene carbonate at 298 K and μ = 0.1 M Et_4NClO_4; drawn from data reported in Ref. [41].

(chart 1) because they are among the most thermodynamically stable lanthanide complexes in addition to being kinetically inert, two conditions crucial to their use in bioanalyses and bioimaging. Commercial contrast agents for magnetic resonance imaging (see figure 5, bottom panel) [47], optical analytical sensors [48–50], stains for cellular signaling and imaging [51], or chiral probes [52] are typical examples of the usefulness of the cyclen-based molecular complexes. Expansion of the macrocycle to produce 14-membered cyclam

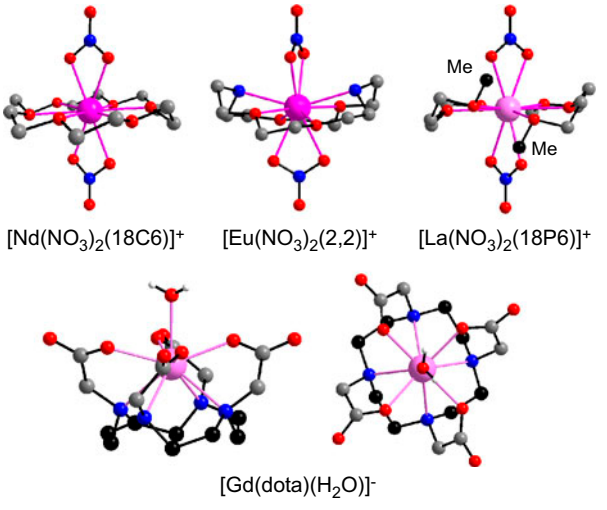

Figure 5. Top panel: influence of added flexibility to a coronand, going from 18C6 to (2,2), on the coordination environment and structure of the corresponding podate; redrawn from data in Refs. [43–45]. Bottom panel: structure of $[Gd(dota)(H_2O)]^-$ showing the encapsulation of the metal ion according to the induced-fit principle (left) and the pseudo-C_4 geometry of the coronate (right); redrawn from data in Ref. [46].

derivatives did not prove as successful as the tailoring of cyclen ligands but, on the other hand, cyclam derivatives are the core of lanthanide dendrimers with remarkable optical properties [53].

Calixarenes (chart 2) have a framework which consists of a platform with two rims onto which functional groups can be separately attached. They are relatively flexible, the number of donor atoms can be modulated and ligating pendant arms can easily be added to fulfill the coordination requirements of the metal ions using, again the induced-fit concept [10]. Their metal complexes provide catalysts for cyclization and polymerization reactions [54]. In addition, separation processes have been proposed with calixarenes containing carboxy-methyl-phosphoryl groups and taking advantage of the rigidifying effect of internal H-bonding [55].

The popularity of macrocyclic Schiff base ligands arises from the template effect discovered at the beginning of the 1980s: large macrocycles can be obtained via one-pot protocols and, in addition, the product of the reaction is often the sought for complex (scheme 1).

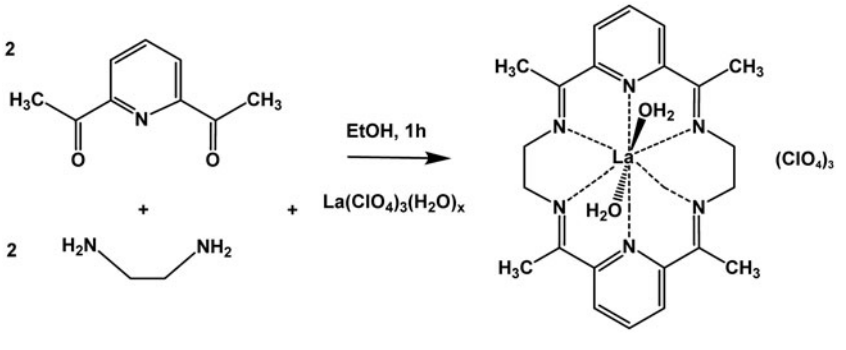

Scheme 1. Template effect of La^{III} in the synthesis of a macrocyclic Schiff base [58].

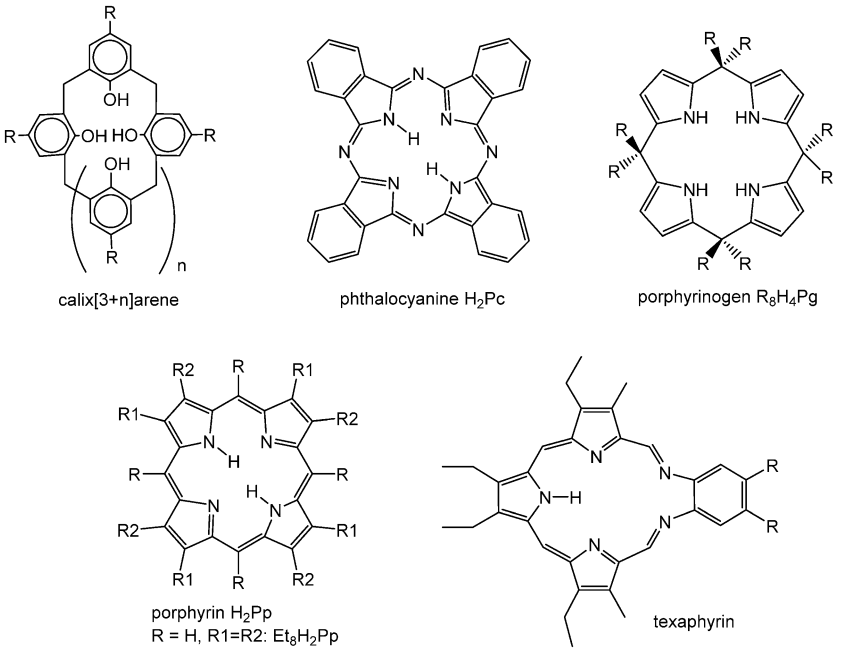

Chart 2. Calixarenes, phthalocyanines and porphyrins.

Polymetallic complexes may also be synthesized in this way, either 4f-4f, 4f-4f′, 4f-5f, or 4f-nd, displaying the full range of luminescent and magnetic properties of the metal ions, as well as mastering metal–metal interactions [38, 56, 57].

Tetrapyrrole derivatives such as porphyrins or phtalocyanines (chart 2) have large delocalized π systems and exhibit a wide range of optical, electrical, magnetic, and spectroscopic properties. Since lanthanide ions have similar properties, their combination with porphyrins and phtalocyanines has been investigated quite early, in the mid-1960s when $Ln(Pc)_2$ complexes (Ln = Pr, Nd, Er, and Lu) were isolated; in contrast, bis(porphyrinato) complexes $Ln(Pp)_2$ were characterized in 1983 only [59]. Since the lanthanide ions are larger than the size of the rings in Pc and Pp complexes, the metal centers are usually located outside the ring. Generally speaking, two main types of complexes have been isolated: (i) 1 : 1 half-sandwiches, in which the coordination sphere of the lanthanide ion is completed by ancillary ligands [60] and (ii) 1 : 2, sandwich compounds (double-decker complexes) in which the metal ions are inserted between two parallel rings [61]. Other stoichiometries include 2 : 2 and 2 : 3 complexes, the latter being referred to as "triple decker" compounds (figure 6). When the ligands are fully de-protonated, either 1 : 1 or 2 : 3 stoichiometries are found while 1 : 2 complexes mainly form with tetravalent cerium. A wide range of applications have emerged from these studies which include electrochromic materials, organic field-effect transistors [62], optical-limiting materials [63], NIR luminescent complexes and sensors [64], photodynamic therapy of cancer for which texaphyrin derivatives were probed [65], catalysis and activation of small molecules (figure 6, right), single-molecule magnets [66] and shift reagents [67].

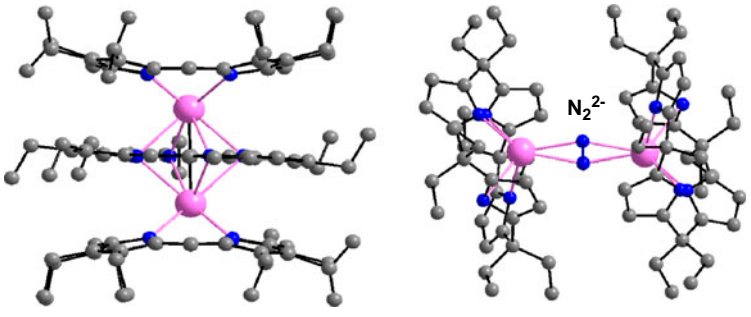

Figure 6. (Left) Triple-decker $[(Ce^{III})_2(Et_8Pp)_3]$ complex redrawn from [59] and (right) activation of dinitrogen by complexation to two Nd^{III} porphyrinogen complexes, redrawn from [68].

5. Supramolecular self-assembled helicates

Supramolecular chemistry is, according to its father, J.-M. Lehn, the chemistry beyond molecules, a chemistry in which large entities are built thanks to weak interactions between molecules, such as hydrogen bonds, π-stacking interactions, dipole–dipole interactions, van der Waals interactions, commonly referred to as non-covalent interactions. Supramolecules extend the field of chemistry to molecular recognition, bringing it close to natural phenomena observed in biology. In the initial context, coordination bonds have been included into non-covalent interactions since one of the early goals of supramolecular chemistry was to selectively recognize and complex a given metal ion, for instance for modeling the potassium/sodium transport through biological membranes. This explains why the border between coordination and supramolecular chemistry is rather thin and why "supramolecular" and associated "self-assembly" are often used to describe what is simply the formation of ion–dipole or ionic bonds between a metal cation and ligand strands (i.e. coordination chemistry). A more restrictive and correct use of these terms would be to limit them to processes in which ligands interact through weak intermolecular forces to build a cavity able to host a specific metal ion. This self-assembly process is then different from a simple step-by-step coordination mechanism in which, for instance, 1 : 1, 1 : 2, and 1 : 3 metal complexes form sequentially, each reaction being characterized by a stepwise formation constant. Alternatively, self-assembly may also characterize the programmed interaction between a metal complex and, for instance, an analyte, or between metal complexes to build larger entities such as capsules or extended networks.

Inspired by the secondary helical structure of proteins and deoxyribonucleic acids induced by non-covalent interactions, chemists have used metal–ligand bonds for programming the connection of helical strands around a central axis, leading to so-called polynuclear helicates [69]. The nanoscopic metal-containing helices are ideal for controlling the magnetic and/or optical properties of one metal ion by the other through interactions along the intermetallic axis. The first lanthanide-containing dinuclear helicate was self-assembled in 1992 from a neutral bis(benzimidazolepyridine) ligand by C. Piguet and collaborators [70] and its structure revealed stabilizing π-staking interactions between the ligand strands and a Ln–Ln distance of about 900 pm (figure 7). The framework of the compartmental ligand was carefully chosen in that the spacer must be rigid enough to transmit the helical twist from one coordinating unit to the other while being flexible enough to allow formation of the helical structure without too many constraints. This scaffold has been the starting

point for the design of a wealth of NNN–NNN and ONN–NNO compartmental ligands. Further extensions implied tri-and tetratopic ligands, as well as reducing the number of donor atoms in one compartment for the binding of d-transition metal ions [71]. The solution structure of homometallic dinuclear lanthanide helicates with C_2-symmetrical ligands, as deciphered from lanthanide-induced NMR shifts [72], is similar to the solid state structure with an average D_3 symmetry. An interesting feature is that the 2 : 3 helicates are quite stable in organic solutions and water despite a large calculated Coulomb repulsion between the two trivalent cations; thermodynamic considerations for 3d-4f and 4f-4f-4f helicates, however, show that the Ln^{III}–Ln^{III} repulsive energy (≈700 kJ mol^{-1}) is largely compensated by solvation energy, explaining the stability of the edifices [73].

Thorough thermodynamics investigations of the formation of the helicates generated a model, the so-called extended site binding model, which reproduces quite well experimental stability constants for the self-assembly of m metal ions with n ligand strands having m binding sites:

$$\beta_{m,n}^{Ln,L} = \omega_{m,n}^{Ln,L} \cdot \prod_{i=1}^{mn} f_i^{Ln} \cdot \prod_{i=1}^{mn-m-n+1} c_i^{\text{eff}} \cdot \prod_{i<j} e^{-\Delta E_{1-2}^{Ln,Ln}/RT} \prod_{k<l} e^{-\Delta E_{1-2}^{L,L}/RT} \tag{4}$$

where $\omega_{m,n}^{Ln,L}$ is the ratio of symmetry numbers of the reactants and products, f_i^{Ln} are the affinities of the metal ions for a given binding site, and $\Delta E_{1,2}^{X,X}$ are the intramolecular interaction energies between two consecutive metal ions (X = Ln) or intermolecular interactions between two ligand strands (X = L); for details, see [71] and cited literature therein.

The initial work on lanthanide helicates has been extended along several avenues. A first one is the design of multicompartmental ligands leading to tri-, tetra-, and even pentanuclear [74] homometallic helicates. A second project involved looking into potential selectivity while reacting different Ln^{III} cations with the compartmental ligands and looking into the generated statistical mixtures, which can be quite complex considering both head-to-head-to-head (HHH) and head-to-head-to-tail arrangements of the ligand strands; some deviations from statistical mixtures were observed, but the relative stability constants $K^{La,Lu}$ deviate little from statistical values, pointing to small heterometallic

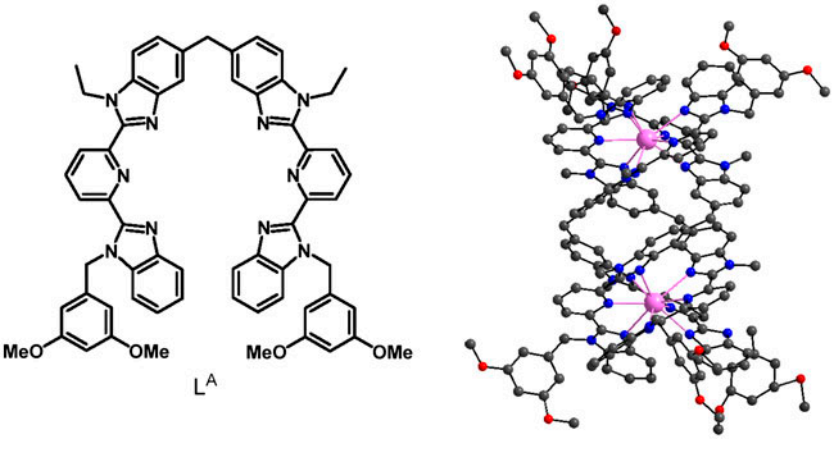

Figure 7. First structurally characterized lanthanide helicate, $[Eu_2(L^A)_3]^{6+}$, redrawn from [70].

discrimination. Introducing dissymmetry in the compartmental ligands in order to emphasize changes in metal–ligand affinities via the formation of different coordination sites leads to much larger size discrimination with, in the case of $[HHH\text{-}LaLu(L^{AB})_3]^{3+}$, the proportion of the La–Lu species reaching 90% as compared to the statistical value of 50% (figure 8). This is due to the larger affinity of the NNO binding unit for the smaller Ln^{III} ions as shown for Eu^{III} by luminescence spectroscopy: the EuN_6 species is much less luminescent than EuN_6O_3 owing to the presence of a quenching charge transfer state [75]. Energy transfer along the Ln–Ln′ axis has also been demonstrated for several pairs of lanthanide ions [71].

A third research topic is concerned with d-f helicates with the main goal of tuning the properties of one metal ion by the other through axial interaction [71]. In view of the high steric requirement of the d-transition metal ions, the $M^{II/III}L_3$ tripod works as a preorganized ligand and facilitates Ln^{III} complexation. For instance, $\log \beta_{23}$ values for the formation of $[HHH\text{-}LaM(L2)_3]^{5+}$ cations (chart 3 in acetonitrile amount to 30 (M = Zn) and 26 (Fe) while the 1 : 3 species have $\log \beta_3$ values equal to 15 (La), 18.8 (Zn), and 20.4 (Fe), pointing to an extraordinary selective self-assembly process.

Heterometallic helicates with divalent Zn, Fe, Cr, Ru, Os, and trivalent Cr have been isolated and displayed highly interesting features. Among them, one is the tuning of the spin-crossover temperature in $[LnFe(Li)_3]^{5+}$ (i = 1, 2). Regarding optical properties, diamagnetic low-spin Fe^{II} in violet $[FeEu(L1)_3]^{5+}$ totally quenches Eu^{III} luminescence, contrary to paramagnetic high-spin Fe^{II} in yellow $[FeEu(L3)_3]^{5+}$ [77]. Moreover, a substantial lengthening of excited-state lifetimes of NIR-emitting lanthanide ions can be achieved by energy transfer from inert Cr^{III} in $[CrLn(L1)_3]^{5+}$ helicates; for Ln = Yb, NIR-luminescence decays with a lifetime equal to that of Cr^{III}, 1.96 ms *versus* 20 μs in the ZnYb helicate (figure 9) [78]. As a follow-up, the tri-compartmental ligand L4 has been programmed for the complexation of two Cr^{III} in the end cavities and of a lanthanide ion in the central binding unit. The 3d-transition metal ions play the role of sensitizers (50% energy transfer efficiency at 10 K)

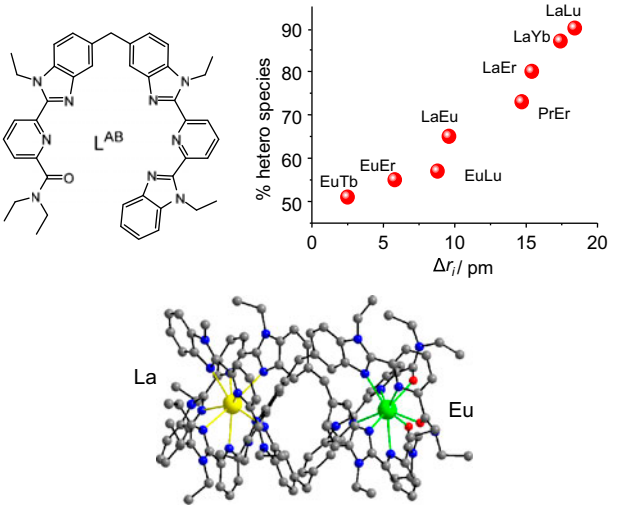

Figure 8. Top: percentage of hetero $[HHH\text{-}LnLn'(L^{AB})_3]^{6+}$ species in acetonitrile, drawn from data reported in [76]. Bottom: crystal structure of $[HHH\text{-}LaEu(L^{AB})_3]^{6+}$; redrawn from [75].

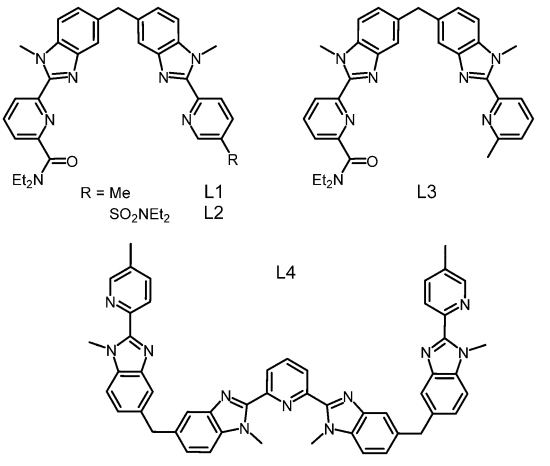

Chart 3. Compartmental ligands for the simultaneous complexation of d and f metal ions.

and when excited in the Cr(^{2}E, $^2T_1 \leftarrow {}^4A_2$) absorption band at 748 nm, green upconverted luminescence from Er^{III} is generated. This is the first demonstration of upconversion in a molecular complex with organic ligands [79].

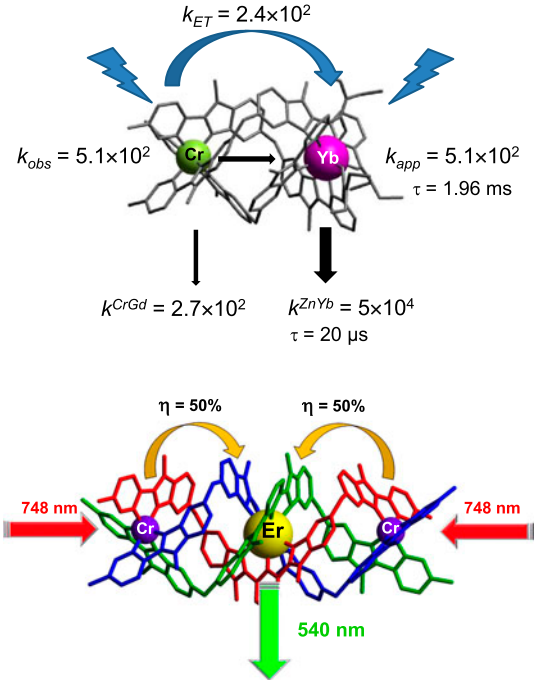

Figure 9. Top: energy migration process in $[CrYb(L1)_3]^{5+}$; rate constants are in s^{-1}, at 10 K; adapted from Ref. [80]. Bottom: molecular upconversion at 10 K in $[Cr_2Er(L4)_3]^{9+}$; data from Ref. [79].

The work described above has been conducted in non-aqueous solvents or in the solid state. However, self-assembly of lanthanide helicates is also feasible in water. For that purpose, carboxylic acid or phosphonic acid coordinating units have been grafted onto the pyridine moiety (see H_2L^{C1}, chart 4). Despite the large de-hydration energy of the aqua ions, neutral and highly stable helical edifices form under physiological conditions (pH 7) that have thermodynamic stability larger than dtpa complexes. The overall solution structure in water is the same as in non-aqueous solvents with the metal ions well protected from solvent interaction. As a consequence, the neutral helicates are highly luminescent with quantum yields of 21 and 11% for $[Eu_2(L^{C2})_3]$ and $[Tb_2(L^{C2})_3]$, respectively [81]. These complexes are non-cytotoxic up to a concentration of 0.5 mM and they stain the endoplasmic reticulum of several cell lines. Further derivatization of the polyoxyethylene side arm allows one to bioconjugate the helicates to streptavidin or to specific monoclonal antibodies. A protocol for the specific detection of biomarkers expressed by human breast cancer cells has been developed and, thanks to time-resolved detection of luminescence, microscopy images, proved to be highly sensitive and reliable [82]. Furthermore, helicates such as $[Eu_2(L^{C5})_3]$ are amenable to multiphoton excitation, opening real perspectives for in-depth tissue imaging [83].

Chirality of the helical architectures is also catching attention. Pure stereoisomers could be isolated for CrEu helicates [84] and several other chiral helicates are now at hand [85–87]. General interest for the self-assembly of lanthanide helicates is presently growing, particularly with respect to thermodynamic control [88] and to computer-aided *de novo* design of such architectures [89].

6. Coordination polymers

CPs, also referred to as metal–organic frameworks (MOFs) when they are porous, are built up from metal ions and multidentate bridging inorganic or organic ligands. Known for a long time, e.g. Prussian blue or metal phosphonates, these materials have seen a surge of interest at the turn of the twenty-first century, thanks to the emergence of nanotechnology. Indeed, nanoporous materials are particularly interesting for size-dependent separations, catalysis, and gas storage. In addition, metal ions confer them physicochemical properties useful in the design of single-molecule magnets, analytical sensors, and non-linear optical

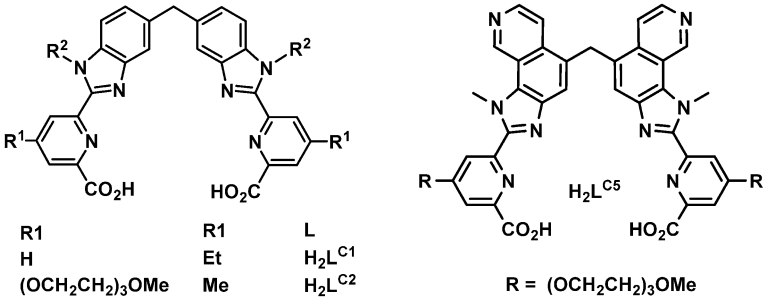

Chart 4. Some ditopic ligands for water-soluble helicates.

or energy-conversion materials. Most of them have organic components resulting in easy processing and film forming. Therefore, MOFs have been tailored as molecular precursors for magnetic-condensed phases, high-temperature superconducting ceramics, or pigments. In this context, lanthanides are particularly interesting in that they are a series of elements with similar chemical properties and ionic radii but with magnetic and optical properties differing considerably from one member of the series to the other. As a consequence, materials with tunable properties can be designed by keeping the organic framework and making an appropriate choice of the lanthanide ion [91]. On the other hand, the lack of steric requirements from these ions renders the synthesis of planned LnMOF structures difficult, a fact reflected by the numerous serendipitous structures with various dimensionalities (1-D, 2-D, and 3-D) reported in the literature, particularly during the past decade. However, a judicious combination of molecular synthesis and crystal engineering helps obtaining a more precise design of functional materials and a given dimensionality, in particular when mixed d-f frameworks are targeted. Porosity can be controlled by using the concept of secondary building units (SBUs): the latter, usually a metal complex or cluster, is connected into extended networks by polytopic linkers, for instance, polycarboxylates. The key is to choose neutral and sufficiently rigid SBUs that serve as large vertices in the MOFs [92]. Luminescence remains the most sought for property for LnMOFs [93] in view of its broad applications in many different fields [94], including the production of barcoded materials [95].

A detailed discussion of lanthanide MOFs here is out of the scope of this mini review; we therefore only outline some facets of this new and exciting aspect of lanthanide (and transition metal) chemistry by describing a few selected examples. Recommendations for the nomenclature of these extended-structure materials call for CP being the most general term; coordination networks are a subset of CP, and MOFs a subset of coordination networks [96].

6.1. *CPs with inorganic ligands*

Cyanide is a simple inorganic ligand which has generated series of valuable *n*d-4f (n = 3–5) magnetic and optical materials. The anion is often bound into a polycyano d-transition metalate such as tetracyanoplatinate, hecacyanocobaltate, or octacyanotungstate [97]; the coordination sphere of the Ln^{III} ion is then completed by another small inorganic (e.g. water and nitrate) or organic (e.g. bipyridine) ligand. One of the advantages of this approach is that mixed Ln MOFs can easily be obtained; one simple example is the 2-D compound $_{\infty}^{2}[LnLn'(H_2O)_5W(CN)_8]$ (LnLn′ = SmTb, EuTb, EuGd), displaying both luminescent and magnetic properties (figure 10, left) [98].

Hydroxide, halogenides, and nitrate are also common bridging inorganic ligands [31]; for instance, several families of hexanuclear hydroxo–nitrato complexes have been identified depending on their hydration. One example is $_{\infty}^{3}[Er_6(\mu_6\text{-}O)(\mu_3\text{-}OH)_8(NO_3)_6(H_2O)_{12}](NO_3)_2 \times 4H_2O$ in which the hexanuclear cores (figure 10, right) are linked together into a complex 3-D network by H-bonds with the interstitial free nitrato groups and crystallization water molecules [99].

Polyoxometalates (POMs) are inorganic anions with a central metallic ion (V, Mo W, less frequently Nb, and Ta) in, usually, its highest oxidation state surrounded by bridging or terminal oxygen atoms. They are divided into two main classes, isopolyanions $[M_xO_y]^{m-}$ and heteropolyanions $[X_xM_yO_z]^{n-}$ where M are the "addenda cations" and X the "primary

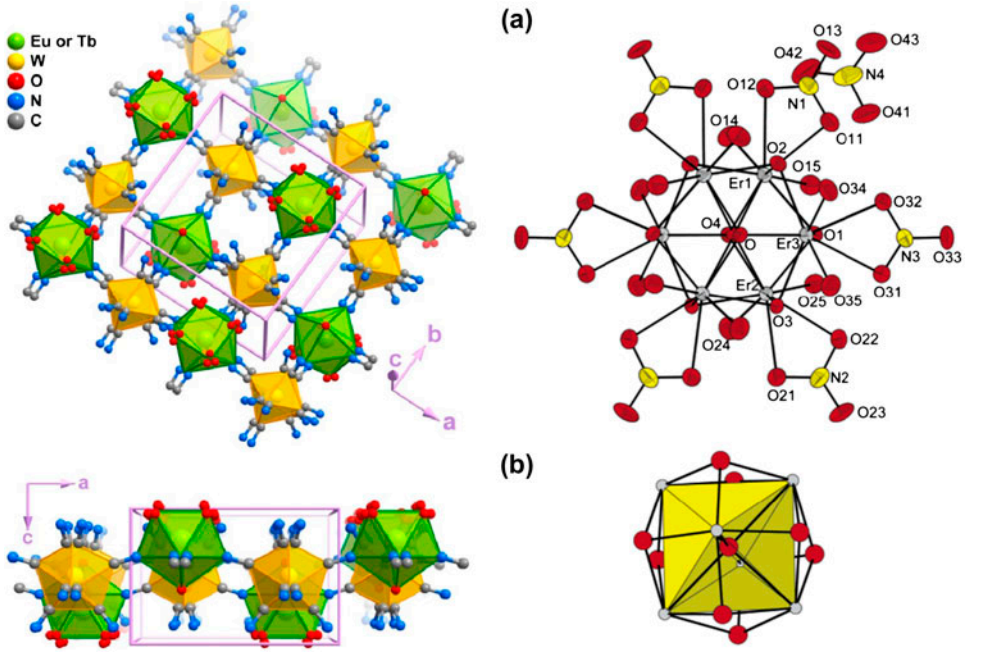

Figure 10. Left: perspective views of $_{\infty}^{2}[EuTb(H_2O)_5W(CN)_8]$; statistical positional disorder is associated with all cyanide anions and most water molecules. Reprinted with permission from Ref. [98], © 2012, American Chemical Society. Right: view of the hexanuclear entity $_{\infty}^{3}[Er_6(\mu_6\text{-}O)(\mu_3\text{-}OH)_8(NO_3)_6(H_2O)_{12}]^{2+}$ (a) with a simplified scheme emphasizing the quasi-perfect Er^{III} octahedron (b). Reprinted with permission from Ref. [99], © 2005, American Chemical Society.

heteroatoms" [30, 100, 101]. Isopolyanions are often unstable while due to the stabilizing effect of X, heteropolyanions are more stable. Archetypes of the most common structures are the Lindquist $[M_6O_{19}]^{m-}$, Anderson $[XM_6O_{24}]^{n-}$, Keggin $[XM_{12}O_{40}]^{n-}$, and Wells-Dawson $[X_2M_{18}O_{62}]^{n-}$ anions which can be modified by removing one or several MO_x groups, resulting in lacunar anions. Unique structures can also been obtained by connecting two or more anions to other metal cations, leading to large networks. In particular, binding of the lacunar POMs to multidentate Ln^{III} cations has resulted in the description of a vast number of new "polyoxolanthanate" (LnPOM) compounds during the past two decades [102]. LnPOMs are often combined with d-transition metal complexes with small ligands (e.g. ethylenediamine, oxalate, and 2,2′-bipyridine) yielding extended edifices. One example is the self-assembled heteropolytungstate anion of trivalent cerium $[Ce_{12}(H_2O)_{36}(AsW_9O_{33})_{12}(WO_2)_4(W_2O_6)_8(W_5CeO_{18})_4]^{76-}$ the elegant D_{2d}-symmetrical structure of which is depicture on figure 11; the disk diameter is approximately 4 nm and Ce^{III} ions are eight- and nine-coordinate [103]. Polyoxolanthanates have been tested for the full range of lanthanide applications: catalysis [104], luminescence for white light emitting diodes [105], contrast agents for magnetic resonance imaging [106], selective binding of radioactive lanthanides [107], or the production of Langmuir–Blodgett films with various physicochemical properties [100]. Remarkably, they may also be inserted into nanoparticles, layered double hydroxides, and various silica frameworks or polymers [100]. There is no doubt that given the huge diversity of these materials they will continue attracting substantial interest.

6.2. *CPs with carboxylic acids*

This class of compounds is very large and owing to the simplicity of the ligands, has been studied during the early stages of the developments of LnMOFs. Structural diversity often arises simply from different numbers of crystallization water molecules since many of these compounds, e.g. with benzene-polycarboxylates, are obtained under solvothermal conditions by slow diffusion through water [90]. A few popular connecting ligands are drawn in chart 5.

Many of these networks have been produced for testing luminescence properties, either for OLEDs or for tagging purposes. One example is $_{\infty}^{3}[Ln_2(bdc)_3(H_2O)_4]$ in which the octacoordinate Ln^{III} ions occupy a single site with pseudo-C_4 symmetry (figure 12, right). The Tb^{III} compound is quite luminescent with a quantum yield reaching 45%, despite the coordination of four water molecules and the luminescence of other lanthanides is also sensitized (Ln = Sm, Eu, Dy). Luminosity is enhanced by diluting the emitter with a non-luminescent ion (Ln = La, Gd, Lu) and the color of trimetallic $La_{2-2x-2y}Eu_{2x}Tb_{2y}$ networks displays a range of different CIE coordinates depending on their composition. Henceforth, this system can be used for producing patterning tags for use in marking or as counterfeiting labels (figure 12, right).

Gas sensing and gas adsorption (separation) are properties which may be built in LnMOFs. For instance, a network assembled from a solvothermal reaction between Yb $(NO_3)_3{\times}5H_2O$ and an organic linker, 5,5′,5″-(benzene-1,3,5-triyl)tris(1-naphthoic acid), yields a network in which the cylindrical 1-D fragment $_{\infty}^{1}[Yb(CO_2)_3]$ functions as rigid SBU. This MOF has pore volumes of about 0.26 $cm^3\ g^{-1}$ and adsorb various gasses in the sequence C_3 hydrocarbons > C_2 hydrocarbons > CO_2 > CH_4 > N_2; consequently, methane can be purified with this porous material from a eight-component mixture [110].

Following the conspicuous discovery in 2004 of single-molecule magnets (SMMs), researchers have rivaled to find adequate systems displaying this property. Since heavy lanthanides have large intrinsic magnetic anisotropy, a factor favoring large energy barriers, they have been under close scrutiny. Here again, wealth of systems has been proposed.

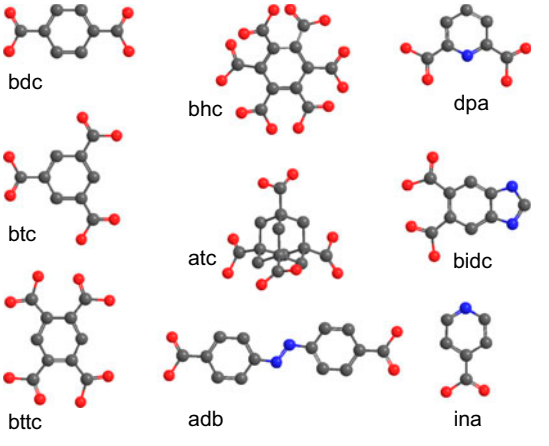

Chart 5. Carboxylate and polycarboxylate ligands often used to build LnMOFs. Key: bdc = benzenedicarboxylate; btc = benzenetricarboxylate; bttc = benzenetetracarboxylate; bhc = benzenehexacarboxylate; atc = adamantanetetracarboxylate; adb = 1,4-azodibenzoate; dpa = 2,6-pyridinedicarboxylate (or dipicolinate); bidc = benzimidazoledicarboxylate; and ina = isonicotinate.

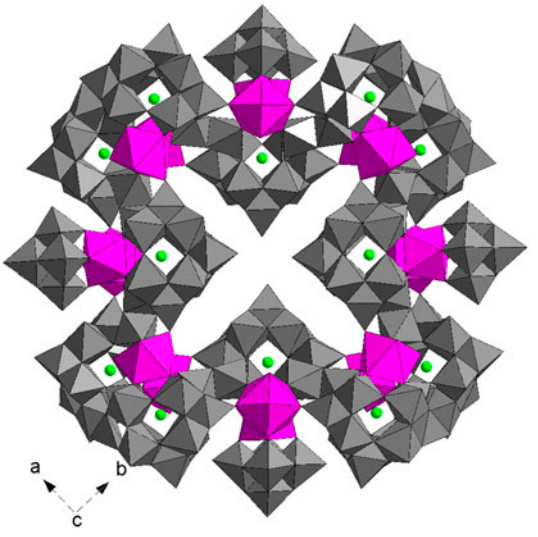

Figure 11. Top view along the $C_2(z)$ axis of the $[(As^{III})_{12}(Ce^{III})_{16}(H_2O)_{36}W_{148}O_{524}]^{76-}$ structure with D_{2d} symmetry. WO_6 polyhedra are drawn in gray, CeO_8 (square antiprism) and CeO_9 (monocapped square antiprism) polyhedra are purple while As^{III} ions are green. Redrawn from the CIF data reported in Ref. [103] (ICSD Nr. 406,326) (see http://dx.doi.org/10.1080/00958972.2014.957201 for color version).

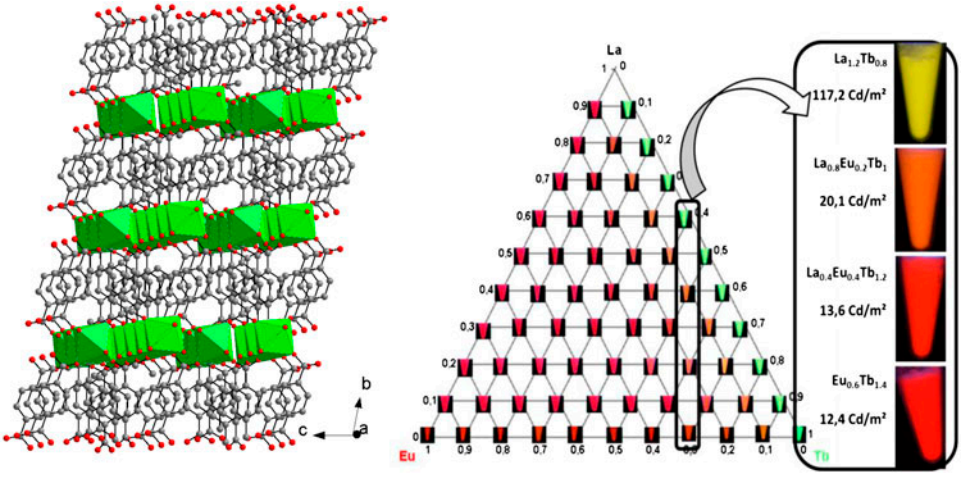

Figure 12. Left: crystal structure of $_\infty{}^3[Tb_2(bdc)_3(H_2O)_4]$ viewed along the axis; TbO_8 polyhedra in green, O atoms in red; redrawn from data reported in Ref. [108] (CIF file: CSD code QACTUJ). Right: pictures under UV irradiation of heterotrimetallic compounds $_\infty{}^3[Tb_{2x}Eu_{2y}La_{2-2x-2y}(bdc)_3(H_2O)_4]$ with 2x and 2y comprised between 0 and 2; reproduced with permission from Ref. [109] © Wiley Interscience 2013 (see http://dx.doi.org/10.1080/00958972.2014.957201 for color version).

About 75% of the works target dysprosium as the favored Ln^{III} ion and CPs have attracted some interest in this field as well because a judicious choice of coordinating linkers favors ferromagnetic interactions [111]. In addition, 3d-4f combination of ions can be easily

programmed in MOFs as in $_{\infty}^{3}\{[Ln_3Co_2(L)_5(HL)(H_2O)_5](ClO_4) \times mH_2O\}$ where L is the 5,5′-dicarboxylate-2,2′-dipyridine anion [112]. Finally, dense 4f-3d MOFs have been synthesized that present a large magnetocaloric effect and sizeable cooling properties, as demonstrated by $_{\infty}^{3}[Gd(HCOOH)_3]$ which outperforms gadolinium gallium garnets. The story only begins [113].

6.3. *CPs with other ligands*

Beta-diketonates are not very stable thermally so that their use has been relatively limited for the design of MOFs until recently. The diketonates are usually provided as SBUs and they are linked to various ligands. The latter can be nitronyl nitroxide radicals in magnetic materials [114] or various polydentate molecules, as in $_{\infty}^{1}[Ln(hfac)_3(L)]$, with L = 1,4-disubstituted benzenes and hfac = hexafluoroacetylacetonate: ternary complexes with 1,4-dimethyltherephtalate are highly luminescent with quantum yields of 51% (Eu) and 56% (Tb); mixing these two ions in various proportions yields materials the color of which can be finely tuned. In addition, the MOFs have good film-forming properties and display triboluminescence [115]. While most of the works on lanthanide CPs relies on screening a variety of compounds to find the ones with exceptional properties, a remarkable study has just appeared in which the authors count on basic statistical mechanics for rationalizing the loading of linear multi(tridentate) polymeric chains with trivalent lanthanides. Similarly to the theory developed in Section 5, the formation of Wolf type II $\{[Ln(hfac)_3]_m(L)\}$ polymers is modeled with only two microscopic parameters: (i) the intrinsic affinity of Ln^{III} ions for the tridentate binding sites of L, f_{N3}^{Ln}, and the intermetallic interactions $\Delta E_{1,2}^{Ln,Ln}$ operating between two occupied adjacent sites. The polymeric ligand L is derived from the tridentate bis(benzimidazole)pyridine scaffold. Selective complexation of Eu^{III} over La^{III} is substantiated by the affinities $f_{N3}^{La} = 3.9(2)$ and $f_{N3}^{Eu} = 56(2)$ calculated from thermodynamic stability constants, while $\Delta E_{1,2}^{Ln,Ln}$ remains almost the same, 1.0(2) kJ mol^{-1} for La and 1.4(2) kJ mol^{-1} for Eu [116]. This approach is promising in view of the rational design of heterometallic lanthanidopolymers in which given metal ions are specifically coordinated to specific coordination sites.

Macrocyclic ligands such as crown ethers [117] or cucurbit[*n*]uril (*n* = 5–14) [118] provide welcome building blocks for MOFs in that the size of their cavity depends on the size of their rings and these guests can then discriminate between hosts with different sizes. Cucurbituril host–guest chemistry is generating broad interest and although until now most of the studies essentially aim at establishing the structure of elaborate networks containing d- or f-metal ions, their functionalities will undoubtedly be exploited in a near future. Indeed, and generally speaking, researchers are more focused on explicit properties they can tailor in MOFs than on specific ligand classes.

7. Hybrid materials

These materials combine a substrate with an active metal ion or complex. They may be broadly divided into sol–gel materials (glasses, silica, and organically modified xerogels), mesoporous and porous materials (silicates and zeolites), polymeric materials, intercalation materials (layered double hydroxides), and nanocomposite materials (nanoparticles). The

lanthanide complexes can be simply doped into the matrix, i.e. held into the framework by weak electrostatic or van der Waals interactions, or covalently linked to it. The field is presently burgeoning and its various aspects are the subject of numerous review articles [119–121], including luminescence thermometry [122].

Three examples are depicted in figure 13 showing different interaction modes between lanthanide complexes and matrices. The first example (a) shows how Ln^{III} complexes with β-diketones are covalently linked to a hierarchically ordered 4,4′-biphenylene mesoporous periodic organosilica framework (PMO); this material conveniently sensitizes the luminescence of Tb^{III}, Er^{III}, and Yb^{III}. The emission color of mixed Ln^{III} materials proved to be tunable by varying the ratio of the metal ions [123]. Non-covalent interaction between a ternary β-diketonate complex and mildly oxidized single-wall carbon nanotube (SWNT) is sketched in second example (b); the same authors have later used tetrakis(β-diketonates) to generate an electrostatic interaction with SWNT and obtained sizeable quantum yields for the Eu^{III}-containing material [124]. In the third example (c), $[Ln(tta)_n]^{(3-n)+}$ units are inserted into the channels of zeolite A, $Na_{96}[(AlO_2)_{96}(SiO_2)_{96}] \times 216\ H_2O$, while $[Ln(L)]^{3+}$ (L = bipyridine, bpy, or phenanthroline, phen) entities are covalently linked onto the surface through 3-(methacryloyloxy)-propyl-trimethoxysilane (γ-MPS) functional groups. To achieve this assembly, sodium ions of the sodalite cage are first exchanged with Ln^{III} ions

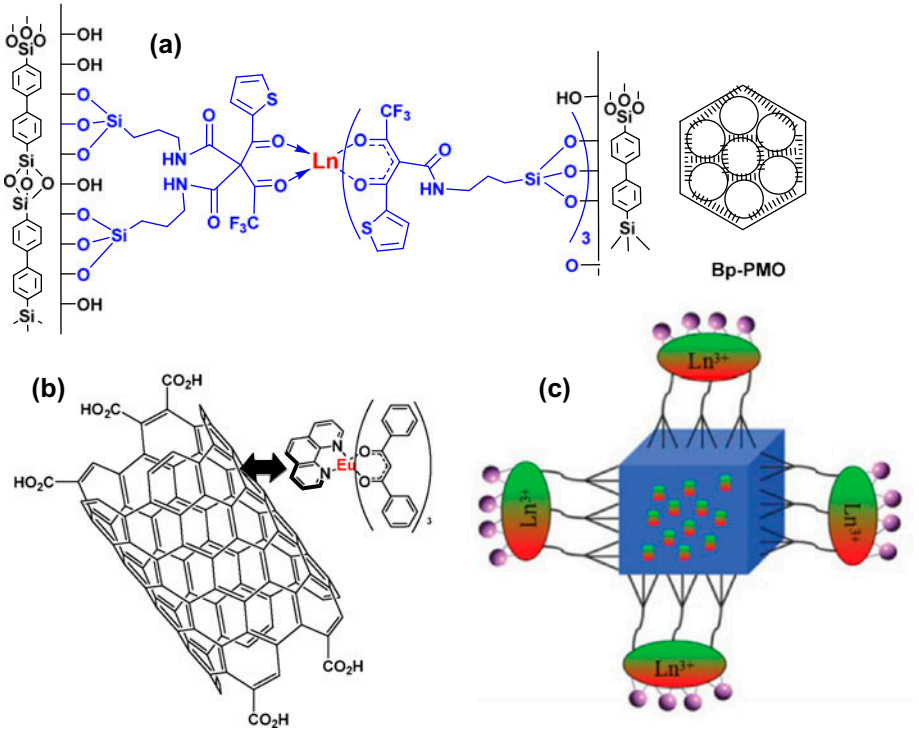

Figure 13. (a) Lanthanide complex with β-diketones doubly covalently bound into a periodic mesoporous silica framework [123]. (b) Non-covalent fixation of a β-diketone ternary complex $[Eu(dbm)_3(phen)]$ (dbm is dibenzoylmethanate) onto the surface of oxidized SWNT [124]. (c) Mixed interactions with zeolite A: $[Ln(tta)_n]^{(3-n)+}$ inserted into the zeolite channels and [Ln(L)-(g-MPS)] complexes on the surface; reprinted with permission from Ref. [125], © 2013, Royal Society of Chemistry.

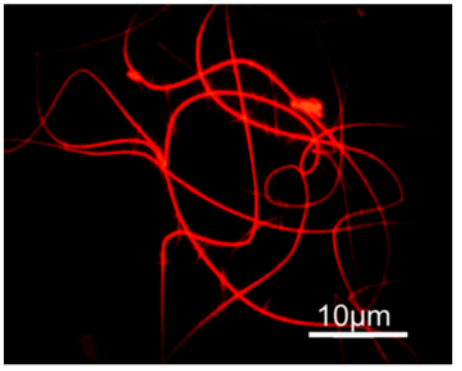

Figure 14. Silica nanoparticles containing [Eu(tta)$_3$(phen)] 2% doped into PMMA and electrospun to produce luminescent nanofibers. Reprinted with permission from Ref. [127], © 2013, Elsevier B.V.

then exposed to vapors of 2-thenoyltrifluoro-acetylacetone (Htta) to form the β-diketonates. In a second step, the zeolite surface is decorated with γ-MPS by reaction with the regularly distributed silanol groups; in turn, the carbonyl group of γ-MPS is coordinated with Ln^{III} ions and the resulting hybrid is finally reacted with vapors of bpy or phen. The matrix itself emits blue light under UV excitation, so that a combination of green-emitting Tb^{III} and red-emitting Eu^{III} ions results in a white-light emitting material potentially adequate for solid-state lighting [125].

When lanthanide complexes are doped into organic polymers such as polymethylmethacrylate (PMMA) some of their properties are enhanced. This is the case for luminescent properties and is due to several factors: (i) a change in refractive index modifies the radiative lifetime that is inversely proportional to the cube of the refractive index; (ii) dilution of luminescent centers into the matrix decreases concentration quenching; (iii) interaction with the matrix can lower the symmetry of the complex and consequently enhance its emission; and (iv) finally, depending on its electronic properties, the polymer sometimes participates in the antenna effect, i.e. in transferring energy onto the luminescent Ln^{III} ion. In addition, doped polymeric materials lend themselves to easy thin-film forming and electrospinning to produce nanofibers [36]. This is well illustrated in figure 14. Luminescent solar concentrators frequently take advantage of these emission enhancements [126].

8. Perspectives

The overview given above, although somewhat superficial, shines light on the vigorous development sustained by lanthanide coordination chemistry during the past decades. In addition to the material presented in the previous sections, other aspects of lanthanide coordination chemistry have also emerged. This is the case of complex formation in and interaction with ionic liquids [128–130], of lanthanidomesogens that are liquid-crystalline materials instilled with the optical and/or magnetic properties of lanthanide ions [131, 132], of metallacrown compounds [133], of gas-phase chemistry which is coming alive thanks to sophisticated mass spectrometry techniques [134], and of organometallic chemistry and catalysis [135, 136].

The quest for materials with enhanced catalytic, optical, and magnetic properties is a driving force for tailoring new sophisticated ligands, extended structures exploiting weak interactions, and, also for investigating unusual redox properties of the lanthanides. Available easy synthetic methods, such as click chemistry, unleash the scientists' imagination and multifunctional molecules, polymers, hybrid materials, and nanoparticles are tackling difficult problems in biosciences and medicine (e.g. theranostics and photodynamic therapy of cancer), energy-related problems (e.g. solar energy conversion), catalysis and photocatalysis (e.g. photodegradation of pollutants), as well as in magnetism (e.g. magnetic refrigeration and single-molecule magnets). Although purely inorganic materials such as phosphors and upconverting nanophosphors are ubiquitous in a great deal of applications, complexes with organic ligands and CPs offer seemingly infinite possibilities for fine tuning of both the binding to lanthanides and the looked-for properties. The emergence of reliable theoretical calculations and thermodynamic models is a plus that will shift purely screening research efforts to more rational molecular construction. As optical and magnetic properties of lanthanide ions are unique and unsurpassed in other elements, a bright future is predicted for the field.

References

[1] P. Thyssen, K. Binnemans. In *Handbook on the Physics and Chemistry of Rare Earths*, K.A. Gschneidner Jr., J.-C.G. Bünzli, V.K Pecharsky (Eds), Vol. 41, Ch. 248, p. 1–94, Elsevier Science B.V., Amsterdam (2011).
[2] J.-C.G. Bünzli. In *Lanthanides, Kirk-Othmer Encyclopedia of Chemical Technology*, p. 1–43, Wiley Online Library (2013). DOI 10.1002/0471238961.1201142019010215.a01.pub3
[3] G.C. Pimentel, R.D. Sprately. In *Understanding Chemistry*, Holden-Day Inc., San Francisco, CA (1971).
[4] F. Nief. In *Handbook on the Physics and Chemistry of Rare Earths*, K.A. Gschneidner Jr., J.-C.G. Bünzli, V.K. Pecharsky (Eds), Vol. 40, Ch. 247, p. 241–300, Elsevier Science B.V., Amsterdam (2010).
[5] M.R. MacDonald, J.E. Bates, J.W. Ziller, F. Furche, W.J. Evans. *J. Am. Chem. Soc.*, **135**, 9857 (2013).
[6] L.C. Thompson. In *Handbook on the Physics and Chemistry of Rare Earths*, K.A. Gschneidner Jr., L. Eyring (Eds), Vol. 3, Ch. 25, p. 209–297, North Holland Publ. Co., Amsterdam (1979).
[7] N. Kaltsoyannis, P. Scott. *The f Elements*, Oxford Science Publications, Oxford (1999).
[8] S. Cotton. In *Lanthanide and Actinide Chemistry*, John Wiley & Sons Ltd, Chichester (2006).
[9] C. Huang. *Rare Earth Coordination Chemistry, Fundamentals and Applications*, John Wiley & Sons (Asia), Singapore (2010).
[10] V.S. Sastri, J.-C.G. Bünzli, V.R. Rao, G.V.S. Rayudu, J.R. Perumareddi. *Modern Aspects of Rare Earths and Complexes*, Elsevier Science B.V., Amsterdam (2003).
[11] J.-C.G. Bünzli, A. Milicic-Tang. In *Handbook on the Physics and Chemistry of Rare Earths*, K.A. Gschneidner Jr., L. Eyring. (Eds), Vol. 21. Ch. 145, p. 306–366, Elsevier Science B.V., Amsterdam (1995).
[12] S.G. Bratsch. *J. Phys. Chem. Ref. Data*, **18**, 1 (1989).
[13] N.B. Mikheev. *Inorg. Chim. Acta*, **94**, 241 (1984).
[14] E.N. Rizkalla, G.R. Choppin. In *Handbook on the Physics and Chemistry of Rare Earths*, K.A. Gschneidner Jr., L. Eyring (Eds), Vol. 15, Ch. 103, p. 393–442, Elsevier Science B.V., Amsterdam (1991).
[15] V. Haase, H.K. Kugler, M. Lehl-Thalinger, U. Trobisch-Raussendorf. In *Gmelin's Handbook of Inorganic Chemistry "Sc,Y,La-Lu"*, Vol. B7, p. 1–23, Springer Verlag, Berlin (1979).
[16] Y. Suzuki, T. Nagayama, M. Sekine, A. Mizuno, Y. Kaoru. *J. Less-Common Met.*, **126**, 351 (1986).
[17] R.D. Shannon. *Acta Cryst.*, **A32**, 751 (1976).
[18] J.D. Xu, E. Radkov, M. Ziegler, K.N. Raymond. *Inorg. Chem.*, **39**, 4156 (2000).
[19] S. Alvarez, P. Alemany, D. Casanova, J. Cirera, M. Llunell, D. Avnir. *Coord. Chem. Rev.*, **249**, 1693 (2005).
[20] H. Zabrodsky, S. Peleg, D. Avnir. *J. Am. Chem. Soc.*, **114**, 7843 (1992).
[21] E.N. Rizkalla, G.R. Choppin. In *Handbook on the Physics and Chemistry of Rare Earths*, K.A. Gschneidner Jr., L. Eyring, G.R. Choppin, G.H. Lander (Eds), Vol. 18, Ch. 127, p. 529–558, Elsevier Science Publ. B.V., Amsterdam (1994).
[22] D.P. Fay, D. Litchinsky, N. Purdie. *J. Phys. Chem.*, **73**, 544 (1969).
[23] C. Cossy, A.E. Merbach. *Pure Appl. Chem.*, **60**, 1785 (1988).
[24] M. Kodama, T. Koike, A.B. Mahatma, E. Kimura. *Inorg. Chem.*, **30**, 1270 (1991).
[25] A.D. Sherry, P. Caravan, R.E. Lenkinski. *J. Magn. Res. Imaging*, **30**, 1240 (2009).

[26] L. Niinistö, M. Leskela. In *Handbook on the Physics and Chemistry of Rare Earths*, K.A. Gschneidner Jr., L. Eyring (Eds), Vol. 9, Ch. 59, p. 91–320, Elsevier Science B.V., Amsterdam (1987).
[27] M. Leskela, L. Niinistö. In *Handbook on the Physics and Chemistry of Rare Earths*, K.A. Gschneidner Jr., L. Eyring (Eds), Vol. 8, Ch. 56, p. 203–334, North Holland Publ. Co., Amsterdam (1986).
[28] Z. Zheng, R. Wang. In *Rare Earth Coordination Chemistry, Fundamentals and Applications*, C. Huang (Ed), p. 229–272, John Wiley & Sons (Asia), Singapore, (2010).
[29] T. Yamase. In *Handbook on the Physics and Chemistry of Rare Earths*, K.A. Gschneidner Jr., J.-C.G. Bünzli, V.K. Pecharsky (Eds), Vol. 39, Ch. 243, p. 297–356, Elsevier Science B.V., Amsterdam (2009).
[30] Y. Lu, E. Wang. In *Rare Earth Coordination Chemistry, Fundamentals and Applications*, C. Huang (Ed), p. 193–228, John Wiley & Sons (Asia), Singapore (2010).
[31] Z. Zheng. In *Handbook on the Physics and Chemistry of Rare Earths*, K.A. Gschneidner Jr., J.-C.G. Bünzli, V.K. Pecharsky (Eds), Vol. 40, Ch. 245, p. 109–239, Elsevier Science B.V., Amsterdam (2010).
[32] R. Wang, Z. Zheng. In *Rare Earth Coordination Chemistry, Fundamentals and Applications*, C. Huang (Ed), p. 91–136, John Wiley & Sons (Asia), Singapore (2010).
[33] A.E. Martell, R.M. Smith. *Critical Stability Constants*, Plenum Press, New York (1974).
[34] K. Binnemans. In *Handbook on the Physics and Chemistry of Rare Earths*, K.A. Gschneidner Jr., J.-C.G. Bünzli, V.K. Pecharsky (Eds), Vol. 35, Ch. 225, p. 107–272, Elsevier Science B.V., Amsterdam (2005).
[35] J.L. Yuan, G.L. Wang, H. Kimura, K. Matsumoto. *Anal. Biochem.*, **254**, 283 (1997).
[36] S. Biju, Y.K. Eom, J.-C.G. Bünzli, H.K. Kim. *J. Mater. Chem.*, **1**, 6935 (2013).
[37] X. Zhang, J. Jiang. In *Rare Earth Coordination Chemistry, Fundamentals and Applications*, C. Huang (Ed), p. 137–192, John Wiley & Sons (Asia), Singapore (2010).
[38] M. Andruh. *Chem. Commun.*, **47**, 3025 (2011).
[39] F. Pointillart, B. Le Guennic, T. Cauchy, S. Golhen, O. Cador, O. Maury, L. Ouahab. *Inorg. Chem.*, **52**, 5978 (2013).
[40] G.A. Kumar, R.E. Riman, L.A.D. Torres, S. Banerjee, A.D. Romanelli, T.J. Emge, J.G. Brennan. *Chem. Mater.*, **19**, 2937 (2007).
[41] J.-C.G. Bünzli. In *Handbook on the Physics and Chemistry of Rare Earths*, K.A. Gschneidner Jr., L. Eyring (Eds), Vol. 9, Ch. 60, p. 321–394, Elsevier Science B.V., Amsterdam (1987).
[42] P. Di Bernardo, A. Melchior, M. Tolazzi, P.L. Zanonato. *Coord. Chem. Rev.*, **256**, 328 (2012).
[43] J.-C.G. Bünzli, B. Klein, D. Wessner, K.J. Schenk, G. Chapuis, G. Bombieri, G. De Paoli. *Inorg. Chim. Acta*, **54**, L43 (1981).
[44] J.-C.G. Bünzli, G.A. Leonard, D. Plancherel, G. Chapuis. *Helv. Chim. Acta*, **69**, 288 (1986).
[45] J.-C.G. Bünzli, J.-M. Pfefferlé, B. Ammann, G. Chapuis, F.-J. Zuniga. *Helv. Chim. Acta*, **67**, 1121 (1984).
[46] C.A. Chang, L.C. Francesconi, M.F. Malley, K. Kumar, J.Z. Gougoutas, M.F. Tweedle, D.W. Lee, L.J. Wilson. *Inorg. Chem.*, **32**, 3501 (1993).
[47] G.J. Stasiuk, N.J. Long. *Chem. Commun.*, **49**, 2732 (2013).
[48] M.L. Cable, J.P. Kirby, H.B. Gray, A. Ponce. *Acc. Chem. Res.*, **46**, 2576 (2013).
[49] S.J. Butler, D. Parker. *Chem. Soc. Rev.*, **42**, 1652 (2013).
[50] J.M. Zwier, H. Bazin, L. Lamarque, G. Mathis. *Inorg. Chem.*, **53**, 1854 (2014).
[51] E.J. New, D. Parker, D.G. Smith, J.W. Walton. *Curr. Opin. Chem. Biol.*, **14**, 238 (2010).
[52] R. Carr, N.H. Evans, D. Parker. *Chem. Soc. Rev.*, **41**, 7673 (2012).
[53] G. Bergamini, E. Marchi, P. Ceroni. *Coord. Chem. Rev.*, **255**, 2458 (2011).
[54] D.M. Homden, C. Redshaw. *Chem. Rev.*, **108**, 5086 (2008).
[55] H. Chu, L. He, Q. Jiang, Y. Fang, Y. Jia, X. Yuan, S. Zou, X. Li, W. Feng, Y. Yang, N. Liu, S. Luo, Y. Yang, L. Yang, L. Yuan. *J. Hazard. Mater.*, **264**, 211 (2014).
[56] P.A. Vigato, S. Tamburini. *Coord. Chem. Rev.*, **248**, 1717 (2004).
[57] W. Radecka-Paryzek. *Can. J. Chem.*, **87**, 1 (2009).
[58] W. Radecka-Paryzek. *Inorg. Chim. Acta*, **45**, 147 (1980).
[59] J.W. Buchler, A. De Cian, J. Fischer, M. Kihn-Botulinski, H. Paulus, R. Weiss. *J. Am. Chem. Soc.*, **108**, 3652 (1986).
[60] D.K.P. Ng. In *Handbook on the Physics and Chemistry of Rare Earths*, K.A. Gschneidner Jr., L. Eyring, G.H. Lander (Eds), Vol. 32, Ch. 210, p. 611–653, Elsevier Science B.V., Amsterdam (2001).
[61] M.M. Ayhan, A. Singh, E. Jeanneau, V. Ahsen, J. Zyss, I. Ledoux-Rak, A.G. Gürek, C. Hirel, Y. Bretonnière, C. Andraud. *Inorg. Chem.*, **53**, 4359 (2014).
[62] J. Jiang, D.K.P. Ng. *Acc. Chem. Res.*, **42**, 79 (2008).
[63] W.K. Wong, X. Zhu, W.Y. Wong. *Coord. Chem. Rev.*, **251**, 2386 (2007).
[64] S. Comby, J.-C.G. Bünzli. In *Handbook on the Physics and Chemistry of Rare Earths*, K.A. Gschneidner Jr., J.-C.G. Bünzli, V.K. Pecharsky (Eds), Vol. 37, Ch. 235, p. 217–470, Elsevier Science B.V., Amsterdam (2007).
[65] O.J. Stacey, S.J.A. Pope. *RSC Adv.*, **3**, 25550 (2013).
[66] D.N. Woodruff, R.E.P. Winpenny, R.A. Layfield. *Chem. Rev.*, **113**, 5110 (2013).
[67] S.P. Babailov. *Prog. Nucl. Magn. Res. Spectrosc.*, **52**, 1 (2008).
[68] E. Campazzi, E. Solari, C. Floriani, R. Scopelliti. *Chem. Commun.*, 2603 (1998).

[69] C. Piguet, G. Bernardinelli, G. Hopfgartner. *Chem. Rev.*, **97**, 2005 (1997).
[70] G. Bernardinelli, C. Piguet, A.F. Williams. *Angew. Chem. Int. Ed.*, **31**, 1622 (1992).
[71] C. Piguet, J.-C.G. Bünzli. In *Handbook on the Physics and Chemistry of Rare Earths*, K.A. Gschneidner Jr., J.-C.G. Bünzli, V.K. Pecharsky (Eds), Vol. 40, Ch. 247, p. 301–553, Elsevier Science, B.V., Amsterdam (2010).
[72] C. Piguet, C.F.G.C. Geraldes. In *Handbook on the Physics and Chemistry and Rare Earths*, K.A. Gschneidner Jr., J.-C.G. Bünzli, V.K. Pecharsky (Eds), Vol. 33, Ch. 215, p. 353–463, Elsevier Science B.V., Amsterdam (2003).
[73] G. Canard, C. Piguet. *Inorg. Chem.*, **46**, 3511 (2007).
[74] B.E. Aroussi, S. Zebret, C. Besnard, P. Perrottet, J. Hamacek. *J. Am. Chem. Soc.*, **133**, 10764 (2011).
[75] N. André, T.B. Jensen, R. Scopelliti, D. Imbert, M. Elhabiri, G. Hopfgartner, C. Piguet, J.-C.G. Bünzli. *Inorg. Chem.*, **43**, 515 (2004).
[76] N. André, R. Scopelliti, G. Hopfgartner, C. Piguet, J.-C.G. Bünzli. *Chem. Commun.*, 214 (2002).
[77] C. Edder, C. Piguet, J.-C.G. Bünzli, G. Hopfgartner. *Chem. Eur. J.*, **7**, 3014 (2001).
[78] S. Torelli, D. Imbert, M. Cantuel, G. Bernardinelli, S. Delahaye, A. Hauser, J.-C.G. Bünzli, C. Piguet. *Chem. Eur. J.*, **11**, 3228 (2005).
[79] L. Aboshyan-Sorgho, C. Besnard, P. Pattison, K.R. Kittilsved, A. Aebischer, J.-C.G. Bünzli, A. Hauser, C. Piguet. *Angew. Chem. Int. Ed.*, **50**, 4108 (2011).
[80] J.-C.G. Bünzli, C. Piguet. *Chem. Soc. Rev.*, **34**, 1048 (2005).
[81] J.-C.G. Bünzli, A.-S. Chauvin, C.D.B. Vandevyver, B. Song, S. Comby. *Ann. New York Acad. Sci.*, **1130**, 97 (2008).
[82] V. Fernandez-Moreira, B. Song, V. Sivagnanam, A.-S. Chauvin, C.D.B. Vandevyver, M.A.M. Gijs, I.A. Hemmilä, H.-A. Lehr, J.-C.G. Bünzli. *Analyst*, **135**, 42 (2010).
[83] J.-C.G. Bünzli. *Interf. Focus*, 3 (2013) Art. Nr. 20130032.
[84] M. Cantuel, G. Bernardinelli, G. Muller, J.P. Riehl, C. Piguet. *Inorg. Chem.*, **43**, 1840 (2004).
[85] C. Lincheneau, R.D. Peacock, T. Gunnlaugsson. *Chem. Asian. J.*, **5**, 500 (2010).
[86] M. Lama, O. Mamula, G.S. Kottas, L. De Cola, H. Stoeckli-Evans, S. Shova. *Inorg. Chem.*, **47**, 8000 (2008).
[87] M. Albrecht, S. Schmid, S. Dehn, C. Wickleder, Z. Shuang, A.P. Bassett, Z. Pikramenou, R. Fröhlich. *New J. Chem.*, **31**, 1755 (2007).
[88] A.M. Johnson, M.C. Young, X. Zhang, R.R. Julian, R.J. Hooley. *J. Am. Chem. Soc.*, **135**, 17723 (2013).
[89] C. Jia, B.P. Hay, R. Custelcean. *Inorg. Chem.*, **53**, 3893 (2014).
[90] O. Guillou, C. Daiguebonne. In *Handbook on the Physics and Chemistry of Rare Earths*, K.A. Gschneidner Jr., J.-C.G. Bünzli, V.K. Pecharsky (Eds), Vol. 34, Ch. 221, p. 359–404, Elsevier Science B.V., Amsterdam (2004).
[91] D.T. de Lill, C.L. Cahill. *Prog. Inorg. Chem.*, **55**, 143 (2007).
[92] M. Eddaoudi, D.B. Moler, H. Li, B. Chen, T.M. Reineke, M. O'Keeffe, O.M. Yaghi. *Acc. Chem. Res.*, **34**, 319 (2001).
[93] J. Heine, K. Muller-Buschbaum. *Chem. Soc. Rev.*, **42**, 9232 (2013).
[94] J.-C.G. Bünzli, S.V. Eliseeva. *Chem. Sci.*, **4**, 1939 (2013).
[95] W.Q. Fan, J. Feng, S.Y. Song, Y.Q. Lei, L.A. Zhou, G.L. Zheng, S. Dang, S. Wang, H.J. Zhang. *Nanoscale*, **2**, 2096 (2010).
[96] S.R. Batten, N.R. Champness, X.M. Chen, J. Garcia-Martinez, S. Kitagawa, L. Ohrstrom, M. O'Keeffe, M.P. Suh, J. Reedijk. *Pure Appl. Chem.*, **85**, 1715 (2013).
[97] M.D. Ward. *Coord. Chem. Rev.*, **251**, 1663 (2007).
[98] E. Chelebaeva, J. Long, J. Larionova, R.A.S. Ferreira, L.D. Carlos, F.A.A. Paz, J.B.R. Gomes, A. Trifonov, C. Guérin, Y. Guari. *Inorg. Chem.*, **51**, 9005 (2012).
[99] N. Mahé, O. Guillou, C. Daiguebonne, Y. Gérault, A. Caneschi, C. Sangregorio, J.Y. Chane-Ching, P.E. Car, T. Roisnel. *Inorg. Chem.*, **44**, 7743 (2005).
[100] C.M. Granadeiro, B. de Castro, S.S. Balula, L. Cunha-Silva. *Polyhedron*, **52**, 10 (2013).
[101] M.T. Pope. In *Handbook on the Physics and Chemistry of Rare Earths*, K.A. Gschneidner Jr., J.-C.G. Bünzli, V.K. Pecharsky (Eds), Vol. 38, p. 337–382, Elsevier Science B.V., Amsterdam (2008).
[102] A. Dolbecq, E. Dumas, C.R. Mayer, P. Mialane. *Chem. Rev.*, **110**, 6009 (2010).
[103] K. Wassermann, M.H. Dickman, M.T. Pope. *Angew. Chem. Int. Ed. Engl.*, **36**, 1445 (1997).
[104] S. Zhao, L. Huang, Y.F. Song. *Eur. J. Inorg. Chem.*, **2013**, 1659 (2013).
[105] J. Cuan, B. Yan. *RSC Adv.*, **3**, 20077 (2013).
[106] W. Chai, S. Wang, H. Zhao, G. Liu, K. Fischer, H. Li, L. Wu, M. Schmidt. *Chem. Eur. J.*, **19**, 13317 (2013).
[107] B.P. Burton-Pye, I. Jones, C.S. Cutler, R.C. Howell, L.C. Francesconi. *Inorg. Chim. Acta*, **380**, 236 (2012).
[108] T.M. Reineke, M. Eddaoudi, M. Fehr, D. Kelley, O.M. Yaghi. *J. Am. Chem. Soc.*, **121**, 1651 (1999).
[109] V. Haquin, M. Etienne, C. Daiguebonne, S. Freslon, G. Calvez, K. Bernot, L. Le Pollès, S.E. Ashbrook, M.R. Mitchell, J.-C.G. Bünzli, S.V. Eliseeva, O. Guillou. *Eur. J. Inorg. Chem.*, **2013**, 3464 (2013).
[110] Y. He, S. Xiang, Z. Zhang, S. Xiong, F.R. Fronczek, R. Krishna, M. O'Keeffe, B. Chen. *Chem. Commun.*, **48**, 10856 (2012).

[111] I.R. Jeon, R. Clérac. *Dalton Trans.*, **41**, 9569 (2012).
[112] M. Fang, P.F. Shi, B. Zhao, D.X. Jiang, P. Cheng, W. Shi. *Dalton Trans.*, **41**, 6820 (2012).
[113] Y.Z. Zheng, G.J. Zhou, Z. Zheng, R.E.P. Winpenny. *Chem. Soc. Rev.*, **43**, 1462 (2014).
[114] R. Liu, C. Zhang, X. Mei, P. Hu, H. Tian, L. Li, D. Liao, J.P. Sutter. *New J. Chem.*, **36**, 2088 (2012).
[115] S.V. Eliseeva, D.N. Pleshkov, K.A. Lyssenko, L.S. Lepnev, J.-C.G. Bünzli, N.P. Kuzmina. *Inorg. Chem.*, **49**, 9300 (2010).
[116] L. Babel, T.N. Hoang, H. Nozary, J. Salamanca, L. Guénée, C. Piguet. *Inorg. Chem.*, **53**, 3568 (2014).
[117] H. Wang, R.M. Wen, T.L. Hu. *Eur. J. Inorg. Chem.*, **2014**, 1185 (2014).
[118] X.L. Ni, X. Xiao, H. Cong, L.L. Liang, K. Cheng, X.J. Cheng, N.N. Ji, Q.J. Zhu, S.F. Xue, Z. Tao. *Chem. Soc. Rev.*, **42**, 9480 (2013).
[119] J. Feng, H.J. Zhang. *Chem. Soc. Rev.*, **42**, 387 (2013).
[120] K. Binnemans. *Chem. Rev.*, **109**, 4283 (2009).
[121] M. Montalti, E. Rampazzo, N. Zaccheroni, L. Prodi. *New J. Chem.*, **37**, 28 (2013).
[122] C.D.S. Brites, P.P. Lima, N.J.O. Silva, A. Millán, V.S. Amaral, F. Palacio, L.D. Carlos. *New J. Chem.*, **35**, 1177 (2011).
[123] S. Biju, Y.K. Eom, J.-C.G. Bünzli, H.K. Kim. *J. Mater. Chem. C*, **1**, 3454 (2013).
[124] J. Mohanraj, N. Armaroli. *The Journal of Physical Chemistry Letters*, **4**, 767 (2013).
[125] J.N. Hao, B. Yan. *Dalton Trans.*, **43**, 2810 (2014).
[126] J.-C.G. Bünzli, A.-S. Chauvin. In *Handbook on the Physics and Chemistry of Rare Earths*, J.-C.G. Bünzli, V.K. Pecharsky (Eds), Vol. 44, Ch. 261, p. 169–281, Elsevier Science, B.V., Amsterdam (2014).
[127] Y.X. Wang, J.G. Tang, L.J. Huang, Y. Wang, Z. Huang, J.X. Liu, Q.S. Xu, W.F. Shen, L.A. Belfiroe. *Opt. Mater.*, **35**, 1395 (2013).
[128] I. Billard. In *Handbook on the Physics and Chemistry of Rare Earths*, J.-C.G. Bünzli, V.K. Pecharsky (Eds), Vol. 43, Ch. 256, p. 213–273, Elsevier Science, B.V., Amsterdam (2013).
[129] A.-V. Mudring, S. Tang. *Eur. J. Inorg. Chem.*, **2010**, 2569 (2010).
[130] K. Binnemans. *Chem. Rev.*, **107**, 2592 (2007).
[131] B. Donnio. *Inorg. Chim. Acta*, **409**, 53 (2014).
[132] K. Binnemans. In *Handbook on the Physics and Chemistry of Rare Earths*, J.-C.G. Bünzli, V.K. Pecharsky (Eds), Vol. 43, Ch. 254, p. 1–158, Elsevier Science, B.V., Amsterdam (2013).
[133] J. Jankolovits, J.W. Kampf, V.L. Pecoraro. *Polyhedron*, **52**, 491 (2013).
[134] J. Marçalo, J.K. Gibson. In *Handbook on the Physics and Chemistry of Rare Earths*, J.-C.G. Bünzli, V.K. Pecharsky (Eds), Vol. 45, Ch. 263, p. 1–110, Elsevier Science, B.V., Amsterdam (2014). in press.
[135] S.M. Guillaume, L. Maron, P.W. Roesky. In *Handbook on the Physics and Chemistry of Rare Earths*, J.-C.G. Bünzli, V.K. Pecharsky (Eds), Vol. 44, Ch. 259, p. 1–86, Elsevier Science B.V., Amsterdam (2014).
[136] W. Huang, P.L. Diaconescu. In *Handbook on the Physics and Chemistry of Rare Earths*, J.-C.G. Bünzli, V.K. Pecharsky (Eds), Vol. 45, Ch. 266, p. 261–329, Elsevier Science, B.V., Amsterdam (2014). in press.